12-12-2017 10:30 AM

A New Single-Phase Single-Stage AC-DC Stacked Flyback Converter With Active Clamp ZVS

Yuntong Li, *The University of Western Ontario*

Supervisor: Dr. Moschopoulos, *The University of Western Ontario*

A thesis submitted in partial fulfillment of the requirements for the Master of Engineering Science degree in Electrical and Computer Engineering

Abstract

Single-stage AC-DC converters integrate an AC-DC front-end converter with a DC-DC back-end converter. Compared with conventional two-stage AC-DC converters, single-stage AC-DC converters use less components and only one controller, which is used to regulate the output voltage. As a result, the cost, size and complexity of AC-DC converters can be reduced, but single-stage converters do not perform as well as two-stage converters, and most have drawbacks that are related to the fact that the DC bus voltage is not controlled an can become excessive.

A new single-phase single-stage AC-DC converter that uses stacked flyback converters is proposed in this thesis. The proposed converter consists of two low power flyback converters stacked on top of each other and an active clamp that helps the main switches operate with ZVS. The stacked structure helps reduce the voltage stresses typical fund in many single-stage converters. In the thesis, the operation of the converter is explained, the steady-state characteristics of the converter are determined and its design is discussed. The feasibility of the new converter is confirmed with experimental results obtained from a 100VAC~220VAC worldwide input, 48V output, 100kHz switching frequency and 200 W output power prototype converter.

Keywords

AC-DC converter, single-stage, single-phase, flyback converter, stacked converter, zero-voltage switching, active clamp

Acknowledgments

At the beginning, I would like to give my gratitude to China Huaxi Engineering Design & Construction Co., LTD, Beijing Company for supporting scholarship to let me pursue my master degree in the University of Western Ontario.

The University of Western Ontario has been a great research institution for my M.E.Sc studies and I would like to acknowledge the tremendous contributions of the university faculty and stuff, which provided a plentiful and unforgettable university experience.

I would like to express my sincere gratitude to my supervisor, Dr. Gerry Moschopoulos, for his patient guidance and continuous support, his motivation and encouragement, his professional training of power electronics knowledge and skills, and his proficient skills of paper writing and publishing. His inexhaustible curiosity for improving technology, his philosophy of research working and his enthusiasm to new things for future trends will keep inspiring me throughout my career. From thinking to accomplishing, from communicating to expressing, his advice was invaluable to me and will be a benefit to me my entire life.

I would like to thank my colleagues in power electronics' lab in UWO - Adel Ali Abosnina, Adel Rajab Alganidi and Javad Khodabakhsh – for sharing their knowledge, encouraging me in my studies, and helping me out.

Part of this research was performed in the ePower lab of Queen's University in Kingston, and I would like to give my thanks to Dr. Praveen Jain for his generosity in accepting me to be a research scholar in his laboratory. I would like to thank Jeananne Vickery for her help around lab. I would also like to thank my colleagues in Kingston - Behnam Koushki Foroush, Cong Wang, Weifeng Gao, Kangping Wang, Wenbo Liu, Chen Yang. Thanks for their work assisting and experimental instructions.

I would like to thank all my friends in London and Kingston that I made outside of my research work for improving quality of my life and bringing me joy.

Lastly but importantly, I would like give my best wishes and thanks to my Mom, Hua Liu, and Dad, Bin Li. I would like to express my gratitude to them in raising me, providing me with a wonderful live, and supporting me in all aspects of mind and life.

Table of Contents

List of Tables

List of Figures

List of Acronyms

AC	Alternative Current
CCM	Continuous Current Mode
DC	Direct Current
DCM	Discontinuous Current Mode
EMI	Electromagnetic Interference
ICS	Input Current Shaper
KCL	Kirchhoff's Current Law
KVL	Kirchhoff's Voltage Law
MOSFET	Metal Oxide Semiconductor Field Effect Transistor
PF	Power Factor
PFC	Power Factor Correction
PWM	Pulse Width Modulation
RMS	Root Mean Square
SSPFC	Single-Stage Power Factor Correction
THD	Total Harmonic Distortion
ZCS	Zero-Current Switching
ZVS	Zero-Voltage Switching

List of Symbols

L_{in}	Input Inductance
L_{lk1}, L_{lk2}	Leakage Inductance
L_{m1}, L_{m2}	Magnetizing Inductance
C_b	Bus Capacitance
C_c, C_{clamp}	Active Clamp Capacitance
C_1, C_2	Bus Capacitors
C_o	Output Capacitor
R_{ds-on}	On-state Resistance
R	Output Resistance
f_{ac}	AC Line Frequency
f_{sw}	Switching Frequency
f_r	Resonant Frequency
f_{sw-aux}	Auxiliary Circuit Switching Frequency
N_1, N_2, N_3	Transformer Turns
N	Transformer Turns Ratio
N_r	Auxiliary Winding Turns Ratio
D_{max}	Peak/Maximum Duty Cycle
V_{ds}	Switch Drain-to-Source Current

V_{rms}	Root Mean Square Voltage
V_{bus}	DC Bus Voltage
$v_{in,k}$	Input Voltage at Interval k
V_{clamp}	Active Clamp Capacitor Voltage
v_{rec}	Rectifier Input Voltage
V_{c1}, V_{c2}	DC Bus Capacitors' Voltage
V_{in}	Input Voltage
V_o	Output Voltage
$V_{ds-peak}$	Peak Value of Switch Drain-to-Source Voltage
I_{rms}^2	Root Mean Square Current
$I_{1,rms}^2$	Root Mean Square of Fundamental current
I_d	Switch Drain Current
I_{Lin}	Input Inductor Current
I_{Lmin}	Minimum Value of Transformer Current
$I_{bus,in-avg}$	Average Value of Current goes into DC Bus
$I_{bus,out-avg}$	Average Value of Current goes out from DC Bus
I_{in-max}	Maximum Value of Input Current
$P_{swtich-loss}$	Switch Power losses
P_o	Output Power

Chapter 1

1 Introduction

Power electronics is the application of power semiconductor devices to convert and control electric power from one form to another. Power electronics, using semiconductor devices as switches, is used in many applications such as mobile phone chargers, laptops power supplies, hybrid vehicles, etc. As power electronics is a comprehensive subject, the power electronics design includes many subjects from electrical engineering such as circuit theory, control theory, electronics, and microprocessors. The main objective of power electronics is to generate required voltage and current output from particular input sources by using power engineering techniques [1].

In power electronics, circuits that convert one type of voltage and current waveform to another type of voltage and current waveform are called converters. The main objective of a converter is to transfer electric power with high efficiency, low cost and small size. Converters that interface source and load can be classified into four different types: AC to DC (rectifier) converter, DC to AC (inverter) converter, DC-to-DC converter and AC-to-AC converter. In addition, power conversion can be implemented with multi-stage converters that combine multiple converters. For example, an AC-DC converter can be implemented with two smaller converter stages with the first stage converting the AC source signal to an intermediate DC signal and the second stage converting the intermediate DC signal to a required DC signal. The AC-DC power converter performs AC-DC conversion and input power factor correction (PFC) in order to comply with harmonic standards such as IEC 1000-3-2 [2] while the DC-DC converter is normally step-up or step-down converter to generate the require voltage. The two-stage AC-DC converter has excellent performance and is thus widely applied in many applications [3]-[14]. It can be considered to be the most popular approach to AC-DC power conversion.

Although two-stage AC-DC converters can have high power factor, low input current harmonic content and regulated DC link voltage, they can be considered to be large and expensive because they require two separate controllers, one for each stage of the

converter. In some applications, low cost and small size is usually the first consideration of converter design; therefore, so-called single-stage AC-DC converters are attractive due to their cost and size advantage. AC-DC single-stage converters combine an AC-DC front-end converter with a DC-DC converter into a single converter that performs both AC-DC and DC-DC power conversion. The DC-DC converter section is typically a flyback or forward converter for low power applications and a half-bridge or full-bridge converter for higher power applications. The AC-DC section is typically a boost converter that also performs input power factor correction (PFC). Most modern AC-DC power converters require input PFC to shape the input current so that it is sinusoidal and in phase with the input AC voltage. Compared with two-stage converters that use two independent converters to perform AC-DC power conversion (an AC-DC and a DC-DC stage), single-stage converters use fewer active switches and only a single controller just for the output voltage as opposed to two separate controllers to regulate the output of two separate converters. As the single-stage converter is cheaper and smaller, but it is not as efficient as two-stage converter [15]-[32].

1.1 AC-DC Power Supplies

AC-DC power supplies are a must in society as most applications require low-level DC voltages but are powered from the AC utility voltage. The field of AC-DC power conversion is thus one that has generated considerable interest among power electronic researchers over the years. In this section, certain fundamentals of the field are explained ahead of a literature review that will be performed in the following section.

1.1.1 Power Factor Correction

AC-DC power supplies have an AC input source with a diode bridge that converts it to a DC voltage. Fig. 1.1(a) shows an AC full wave rectifier suppling a resistive load. The input voltage and current waveforms are presented in Fig. 1.1(b). Since the diodes conduct for only very short amount of time during each AC line cycle, the resulting input current is very non-sinusoidal and the converter thus has a low input power factor. In order to quantify the non-sinusoidal property of the input waveform, total harmonic distortion is

used. This is the ratio of the RMS value of all non-fundamental frequency terms to the RMS value of the fundamental frequency term, which can be expressed as follows:

$$THD = \sqrt{\frac{I_{rms}^2 - I_{1,rms}^2}{I_{1,rms}^2}} \tag{1.1}$$

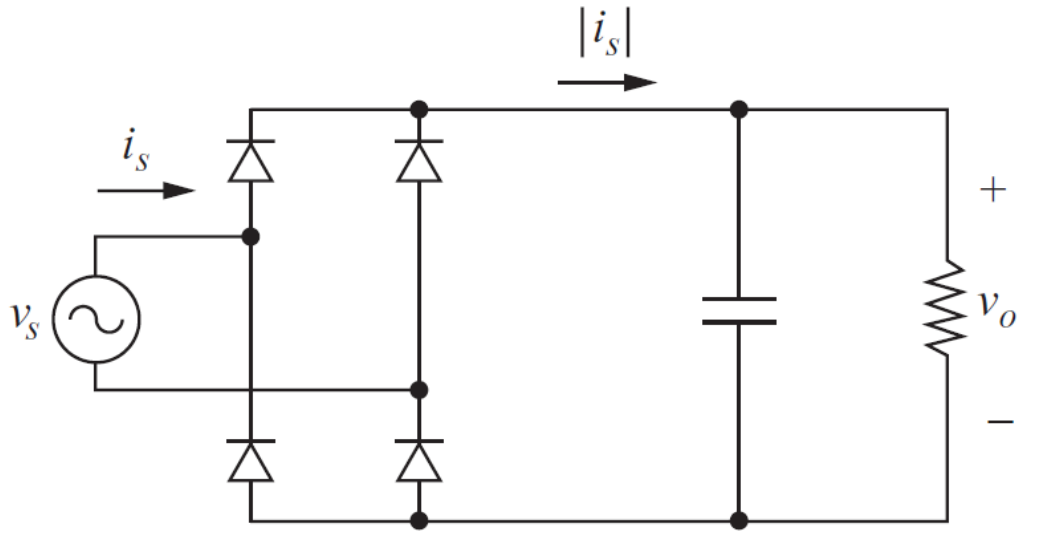

(a)

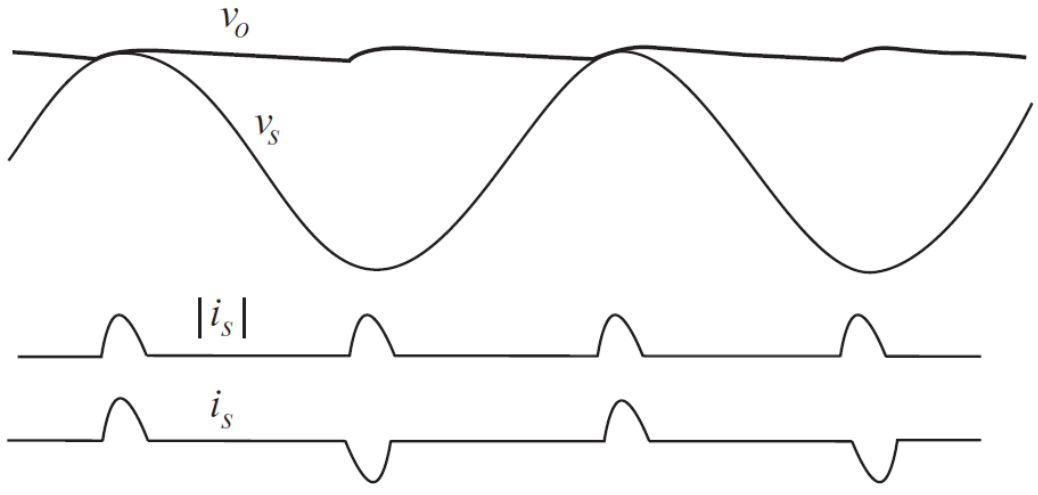

(b)

Figure 1.1: (a) AC fullwave rectifier. (b) Input voltage and current waveform [1].

A common way to improve the power factor is to equip a power factor correction (PFC) Fig. 1.2(a) shows a boost converter used as a PFC converter. The boost converter shapes the input current so that it is sinusoidal and in phase with the input voltage. The converter operates as follows: When the switch is closed, the current in the input inductor will rise; when the switch is opened, the current in the input inductor will fall. Based on the input current rise and fall times, the input inductor current can be made to have a sinusoidal shape. Two types of input inductor current are shown in Fig. 1.2(b) and Fig. 1.2(c): continuous-current mode (CCM) in Fig. 1.2(b) and discontinuous-current mode (DCM) in Fig. 1.2(c). CCM current is used for high-power applications while DCM current is used for low-power applications. The different between CCM and DCM is that current in the input inductor of DCM falls to zero at the each of each switching cycle as the input voltage is low while this is not the case for CCM. Regardless of which approach is used, the output of a boost PFC converter is a high DC voltage that is typically about 400V [1], [22]-[26].

1.1.2 Soft-Switching Techniques

For conventional DC-DC and AC-DC converters, the converter switches generate conduction losses when operated. Before the switch is ON, there is a drain-to-source voltage V_{ds} across the switch. When the switch is ON, the drain current I_d rises in the switch device (typically a MOSFET), which results in conduction loss $P_{swtich-loss} = V_{ds} \cdot I_d$. Before the switch is OFF, drain current exists in the MOSFET. When the switch is OFF, there is a short time during which the drain current falls to zero and the drain-to-source voltage is increased; switching losses are produced. This phenomenon is called hard-switching and typical hard-switching switch voltage and current waveforms are shown in Fig. 1.3(a). The shadow area shows the switching losses of switch operation.

For high frequency converters, switching losses can be excessive and can significantly reduce converter efficiency. In order to reduce these losses, converters are usually operated with zero-voltage switching (ZVS) or zero-current switching techniques (ZCS) such as resonant circuits, active clamp converters, etc. The basic principle of ZVS or ZCS is that the converter eliminates either switch voltage or switch current during the time of a switching transition as dissipated power is related to the product of voltage and current. This results in a significant reduction in switching losses. ZVS and ZCS are specific types

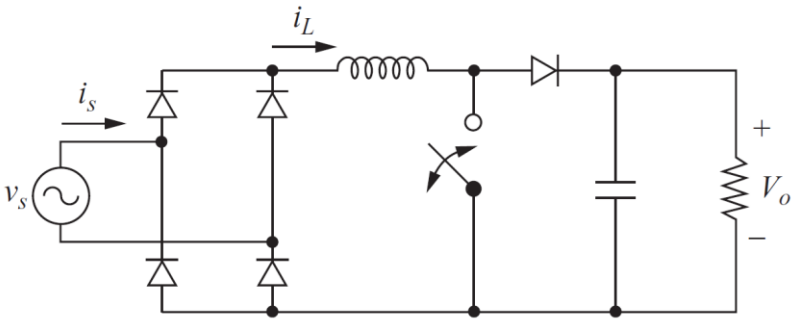

(a)

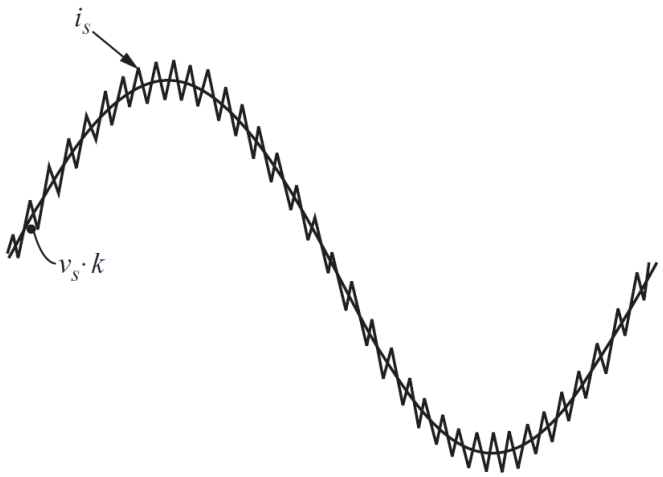

(b)

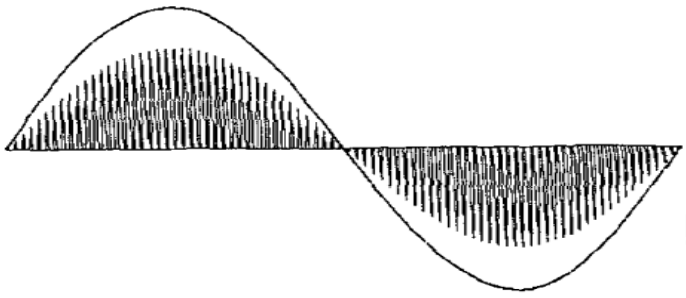

(c)

Figure 1.2: (a) Boost-type power factor converter. (b) Input voltage and input inductor current waveform in continues current mode (CCM). (c) Input voltage and input inductor current waveform in discontinues current mode (DCM) [1].

of what is generally called soft-switching techniques as opposed to hard-switching techniques. An example of switch current and voltage waveforms when soft-switching is

used is Fig. 1.3(b) in order to illustrate the switching loss area that is reduced or eliminated by using soft-switching techniques [1], [27]-[32].

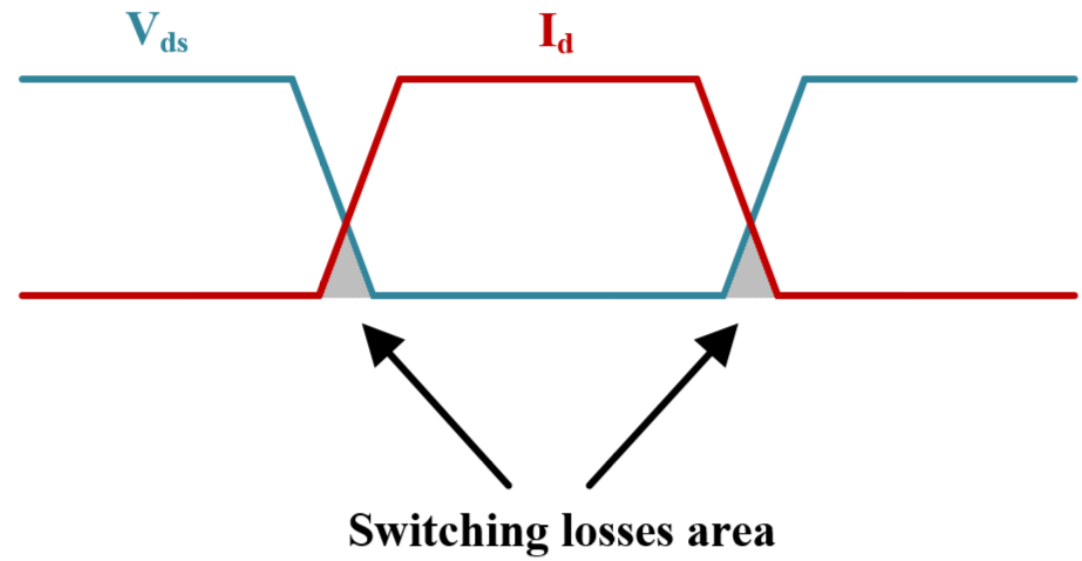

(a)

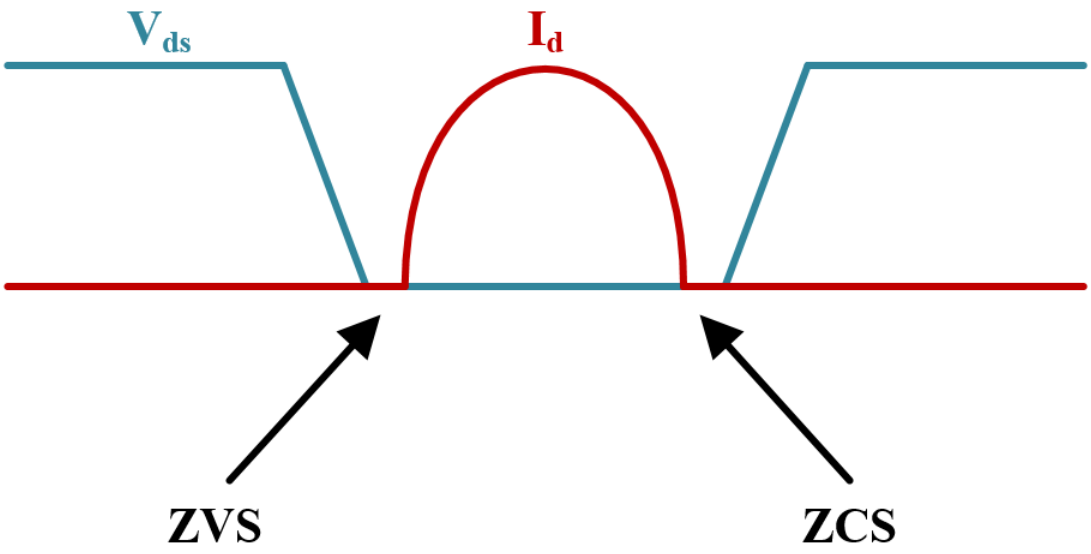

(b)

Figure 1.3: Voltage and current waveforms of (a) hard-switching and (b) soft switching.

1.2 Literature Review

A literature review of state- of-the-art low power AC-DC converters is performed in this section. Several types of recent low power AC-DC single-stage single-phase converters (< 250 W) are presented [33]-[48] and higher power single-stage converters such as the ones proposed in [49] and [50] will not be discussed. For each converter type, its basic principles are discussed and the operation of an example converter is briefly explained along with its strengths and drawbacks.

1.2.1 Conventional Single-stage Flyback Converter without DC Bus Capacitor

Low power single-stage AC-DC converters can generally be classified as belonging to one of two types:

- Converters without a DC bus capacitor.
- Converters with a DC bus capacitor.

The first type of converter is discussed in this section while the second type will be discussed in the next section.

The converter in Fig. 1.4(a) is a flyback converter with a rectified AC input instead of a DC source. The way this converter works is that input current rises when the converter switch is ON and falls when the converter switch is OFF. If the converter's duty cycle is kept fixed throughout the AC input line cycle, then a discontinuous input current consisting of triangular portions with varying peaks such as what is shown in Fig. 1.4(b) will be produced. This waveform is bounded by a sinusoidal envelope so that it is essentially a sinusoidal waveform with high frequency harmonics. If these harmonics are filtered out, then the resulting waveform will be a sinusoidal AC input current waveform.

Converters such as the one shown in Fig. 1.4(a) are simple and inexpensive. They do, however, have the following drawbacks:

- The only filtering that these converters have is at the output – there is no filtering at their primary side as there is no DC bus capacitor. As a result, a large 120 Hz low

frequency AC component can appear at the output. In order to filter out this component, the output capacitor must be larger, which can slow down the response of the converter as well as take up space.

- Hold-up time is a feature that is required in many AC-DC power supplies. Hold-time is defined as the amount of time a converter can still provide a regulated output after an AC failure. Converters such as the ones shown in Fig. 1.4(a) that do not have a DC bus capacitor must rely on just the output capacitor to provide hold-time operation, which means that the output capacitor must be large. This results in the same issues that were described above.

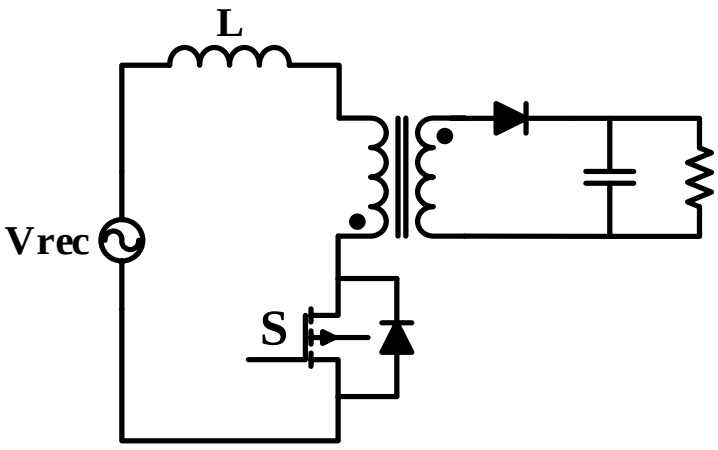

(a)

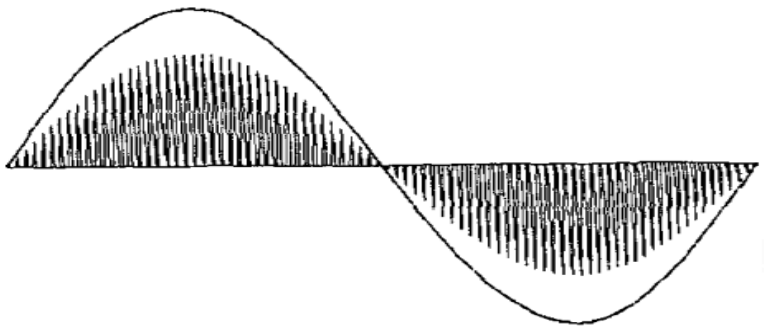

Figure 1.4: (a) Basic single-stage flyback converter. (b) Input voltage and current waveforms.

1.2.2 Basic Single-stage Low Power Converters with DC Bus Capacitor

The converter shown in Fig. 1.5 was first proposed in [32], which is considered to be a landmark paper in the field of single-stage converters as it was among the first, if not the first, to investigate low power single-stage converters of this type. This converter can be synthesized from two-stage converters by combined an AC-DC boost front-end converter with a DC-DC flyback converter then eliminating all redundant and unnecessary elements. They are operated using just a single controller to regulate the output voltage.

The converter shown in Fig. 1.5 operates as follows: When the switch is ON, the output voltage of the input diode bridge rectifier is placed across the input boost inductor and DC bus voltage is applied on the primary side of the transformer simultaneously. The input current rises while energy is stored in the transformer. When the switch is OFF, the current in the input inductor drops as it flows through the DC bus capacitor while the energy stored in transformer is transferred to the output.

The converter is operated with fixed duty cycle. If the input inductor is designed so that the input current is discontinuous throughout the AC input line cycle, then the input current will consist of a set of triangles that is bounded by a sinusoidal envelope, much like the waveform shown in Fig. 1.4(b).

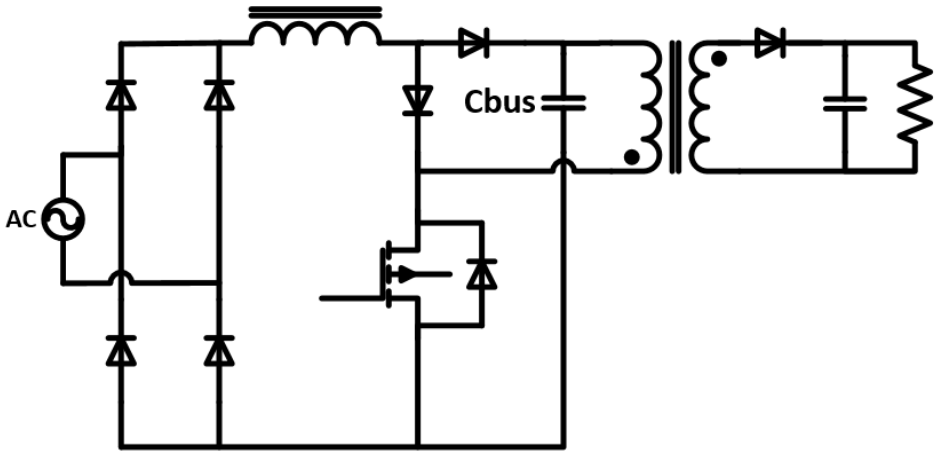

Figure 1.5: Basic single-stage AC-DC flyback converter with DC bus capacitor.

The presence of a bulk capacitor at the DC bus of the primary side of the converter eliminates the drawbacks that exist in single-stage converters like the one shown in Fig. 1.4(a). The DC bus capacitor helps reduce the low frequency 120 Hz harmonic component that is in the input diode bridge rectifier output voltage so that it does not appear at the converter's output; this allows for a smaller output capacitor to be used. Moreover, the DC bus capacitor can be sized to extend hold-up so that any such requirement is met.

1.2.2.1 DC Bus Voltage Reduction Methods

Although the converter in Fig. 1.5 is very simple, it has one important drawback - there is no control over the intermediate DC bus voltage (i.e. voltage across C_{bus} in Fig. 1.5) as there is only one controller. The DC bus voltage can become excessive under certain operating conditions such as high input line / light-load, which necessitates the use of high voltage rated components that can increase cost and high voltage capacitor that can increase size. This especially true if the converter need to operate with universal input line range (86 V_{rms} – 264 V_{rms}).

There are several methods by which the DC bus voltage of basic single-stage converters such as the one shown in Fig. 1.5 can be reduced. Each method involves changing the energy equilibrium at the DC bus. This energy equilibrium is the equilibrium of energy that must exist at the DC bus capacitor when the converter is operating under steady-state conditions and can be stated as follows:

The energy that is delivered to the DC bus capacitor from the input must be equal to the energy that is delivered by the capacitor to the output. If net energy is delivered to the capacitor from the input or from the capacitor to the output, then the converter is not operating in steady-state as the DC bus capacitor voltage has a net charge and its voltage is increasing or it has a net discharge and its voltage is decreasing.

The DC bus voltage reduction methods include the following:

- *Reducing the transformer turns ratio:* This increases the primary side current, which allows more energy to be discharged by the capacitor. The steady-state energy equilibrium is therefore changed so that the DC bus voltage is reduced. Doing this,

however, creates several problems that are a result of the increased primary current. These include higher conduction losses, higher turn-off losses and a narrowing of the converter's duty cycle range of operation.

- *Increasing the input boost inductor:* This reduces the amount of energy that is stored in the inductor when the switch is turned on. Doing so affects the energy equilibrium at the DC bus as less energy stored in the inductor results in less energy being transferred to the DC bus for the same amount of duty cycle. This results in lower DC bus voltage. The main drawback to this approach is that increasing the input inductor can cause the waveform to become distorted, as shown in Fig. 1.6. This is because the input current may no longer be discontinuous throughout the entire AC line cycle, but may become "semi-continuous" with regions where the input current is continuous. As a result, the input current harmonic content may become such that regulatory agency standards on harmonic content are not met, which would be unacceptable from a commercial point of view.
- *Decreasing the magnetizing inductance in flyback converters or the output inductor in forward converters:* This results in more current being drawn from the DC bus capacitor, thus changing the energy equilibrium so that the steady-state DC bus voltage is lower. Doing so, however, means that there will be higher peak currents at the

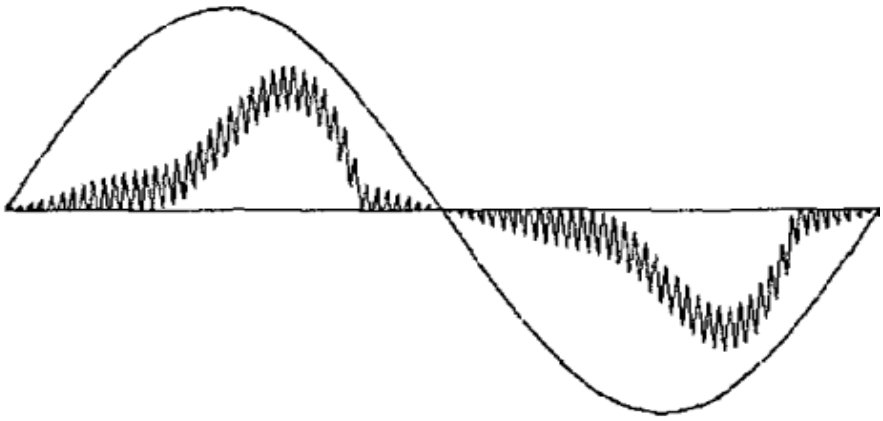

Figure 1.6: Distorted semi-continuous input current waveform.

primary and at the secondary, thus increasing switch stress. Conduction losses may also be increased as the amount of current circulating in the converters is increased.

1.2.3 Review of Recent AC-DC Single-Stage Converter Topologies without DC Bus Capacitor

Research on low power single-stage converters over the past 20 years has focused on trying to improve their operation and performance by overcoming the drawbacks that have been discussed above. As a result, many single-stage converter topologies have been proposed over the years, each with its advantages and disadvantages. In this section of the thesis, several of the most recent types are presented, with the operation of each type explained using an example converter and its advantages and disadvantages stated.

1.2.3.1 Interleaved Converters

Interleaving power converters is a popular approach in power electronics. It involves connecting multiple converters in parallel then operating these converters so that there a 360°/n (where n is the number of converter modules) phase-shift between the two converters. For example, if two converter modules are interleaved, then the phase-shift between the two converters is 180°; if there are three modules, then the phase-shift is 120°.

In general, the main advantages of interleaving are:

- Reduction of current ripple in the input or the output, depending on which section of the converter is interleaved. Interleaving increases the effective switching frequency by n times so that filtering high switching frequency harmonic components becomes easier.
- Reduction of current stress of individual components (switches and diodes) as power is distributed among several converters.

In Fig. 1.7(a), an interleaved single-stage single-phase AC-DC converter is shown [34]. It is implemented with two paralleled flyback converters. It should be noted that capacitor C_b connected to the DC bus is not a bulk capacitor, but is a small capacitor that is used as a snubber to interface the input inductor with the two transformers. It can be discharged whenever a switch is ON.

The converter operates as follows: During the first half of the switching cycle, S_1 is turned ON at the start and current in transformer T_1 rises and is eventually equal to the input inductor current. The input current rises as energy is stored in T_1. S_2 is OFF during this time. When S_1 is turned OFF, the input inductor current is gradually transferred to the small DC bus snubber and falls while energy is transferred to the output. At the start of the second half of the switching cycle, S_2 is turned ON while S_1 is kept OFF and the operation of the

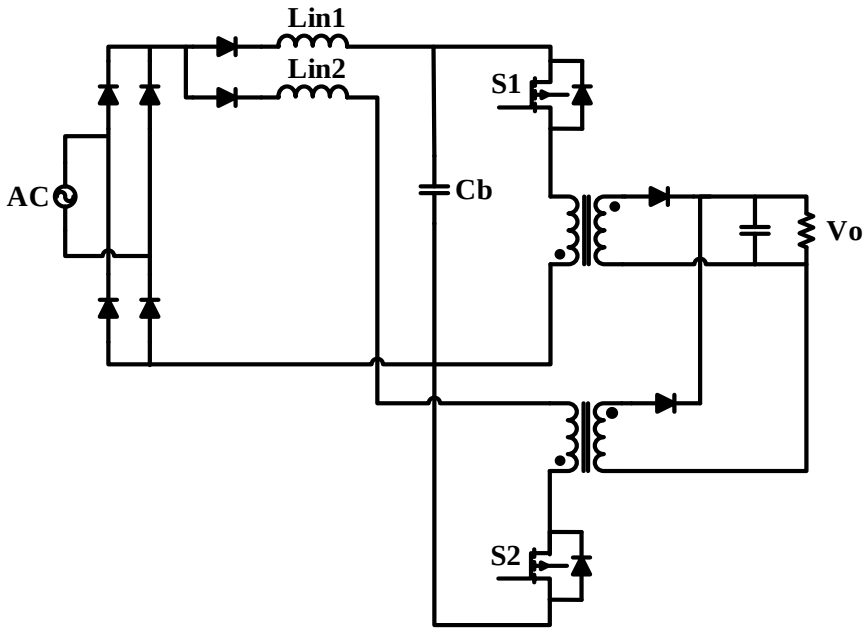

(a)

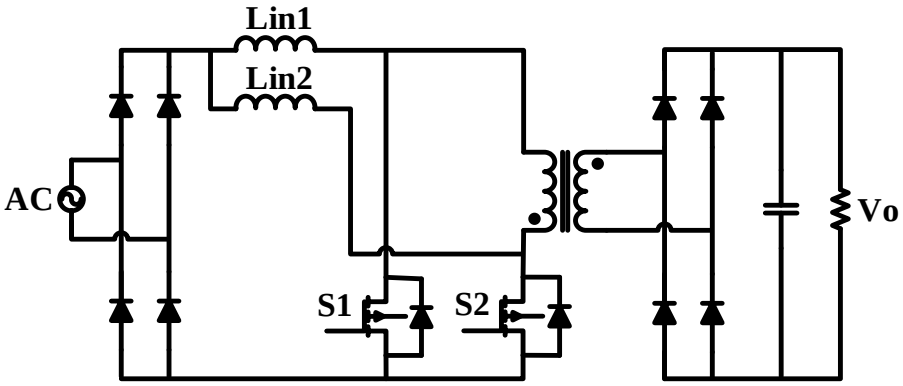

(b)

Figure 1.7: Interleaved single-stage converters. (a) Flyback (b) Current-fed push-pull.

converter becomes the same as in the first half of the cycle except that S_2 and T_2 have current flowing through them instead of S_1 and T_1.

In Fig. 1.7(b), another interleaved AC-DC converter is shown [36]. This converter is based on the current-fed push-pull topology and uses just one transformer instead of just two. Otherwise, the general operating principle of the converter is very similar to the one shown in Fig. 1.7(a).

Although interleaving multiple converters has the above-mentioned advantages, it also has several drawbacks. One is cost as several converters are needed. Another is if the converter is implemented with some sort of soft-switching technique that requires an auxiliary circuit such as the active clamp method, then an additional switch must be added to each converter module, thus further increasing costs.

1.2.3.2 Forward-Flyback Converters

One of the drawbacks of simple forward converters is that their maximum duty cycle is typically limited to 50% in order to allow for sufficient time to reset the transformer. Although it is possible to extend the duty cycle past 50%, it is generally avoided except for some low-line voltage applications due to an increase in the peak switch voltage stress. As a result, no power is transferred to the output for half the switching cycle. This impacts the design of the transformer and can lead to higher primary-side currents.

If a forward converter is implemented in such a way so that the tertiary winding that is used to reset the transformer is connected to the secondary instead of the primary, then a forward converter can allow for energy to be transferred to the output when the switch is OFF. Fig. 1.8(a) shows just such an implementation with a passive snubber connected to the converter switch [37].

The main drawback with this approach is that the output current ripple is increased due to the contribution of current from the flyback winding. This current introduces a low 120 Hz frequency component to the output that increases the size of the output capacitor needed to filter out harmonic components to ensure a DC output. This 120 Hz component comes from the rectified input diode bridge output voltage.

One way to resolve this problem is to use a small converter at the secondary to inject current into the output capacitor whenever the input voltage is near one of its zero-crossings. Such an approach is shown in Fig. 1.8(b) [38]. In this converter, a small buck converter is connected between the forward winding output capacitor and the converter output capacitor. The duty cycle of the small buck converter is increased when the input voltage is near a zero-crossing to inject more current into the output and decreased when the input voltage is close to its peak to inject less. Although this method is effective in reducing output filter capacitor size, its main drawback is the need for a second converter whose operation must be tied to the main converter so that the voltage can be properly regulated. This leads to increased cost, size and complexity.

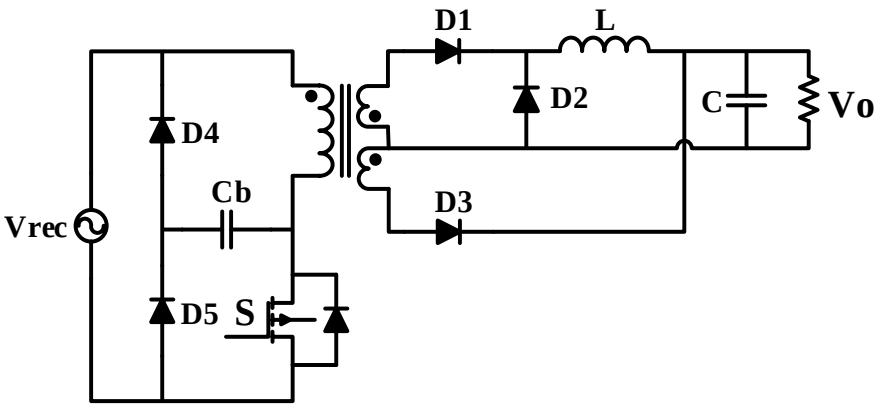

(a)

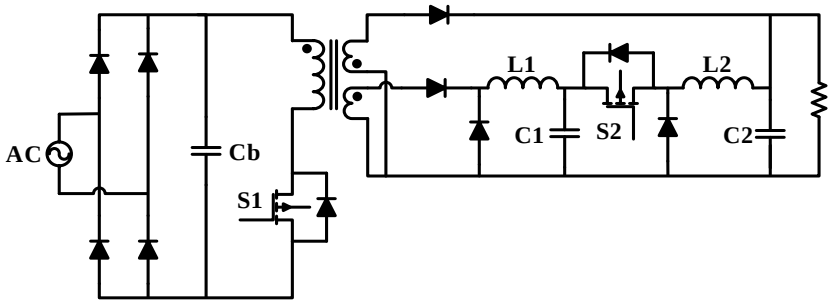

(b)

Figure 1.8: Forward-flyback single-stage converters. (a) Converter with basic secondary topology. (b) Converter with secondary buck converter.

1.2.4 Review of Recent AC-DC Single-Stage Converter Topologies with DC Bus Capacitor

Recent AC-DC single-stage converters with a bulk DC bus capacitor in their topologies are discussed.

1.2.4.1 Single-Stage Converter with Counter Voltage

As explained in Section III, the energy equilibrium at the DC bus can be changed if either the amount of energy delivered from the input to the DC bus capacitor or the amount of energy delivered to the output from the DC bus capacitor is changed. One way by which the amount of energy from the input can be changed (i.e. reducing the amount of energy stored in the input inductor and ultimately transferred to the DC bus for the same duty cycle) is by introducing a counter voltage to one end of the inductor so that when the switch is turned ON, less energy is stored in the inductor and thus less energy is transferred to the DC bus capacitor.

Many ways have been proposed to implement this counter voltage; several examples are shown in Fig. 1.9. The flyback converter shown in Fig. 1.9(a) uses an auxiliary winding taken from the converter transformer as a 'magnetic switch', operating like a boost converter switch [39]. When the switch is ON and energy is being stored in the transformer, a negative voltage is placed across the auxiliary winding, which cancels out some of the voltage of the capacitor that it is connected to, thus allowing the input current to rise. When the switch is turned OFF, energy stored in the transformer is released to the output and the auxiliary winding reverses polarity so that it exceeds the amplitude of the input voltage. This causes the input inductor current to fall and it eventually falls to zero sometime during this part of the switching cycle. Another way to impress a counter voltage is shown in Fig. 6(b) [10]. This converter is the same as the converter shown in Fig. 1.5 in Section 1.2.2 except that capacitor C_1 has been added between the input inductor and switch. This capacitor keeps the full input voltage from being impressed across the inductor when the switch is turned ON.

The main drawback with single-stage converters with magnetic switches is that the input current may become distorted, as shown in Fig. 1.9(c) [42]. This input current distortion is

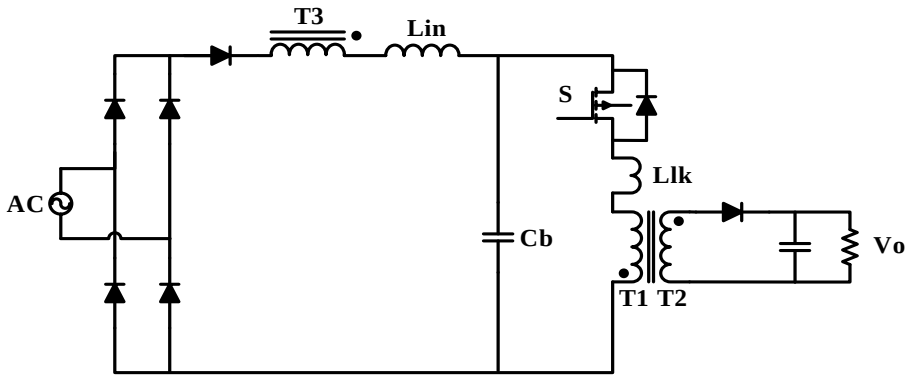

(a)

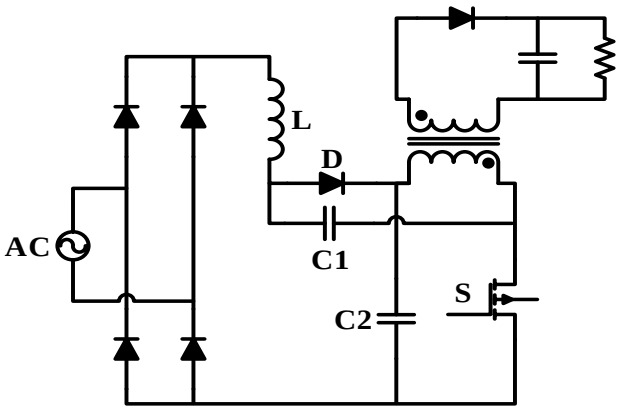

(b)

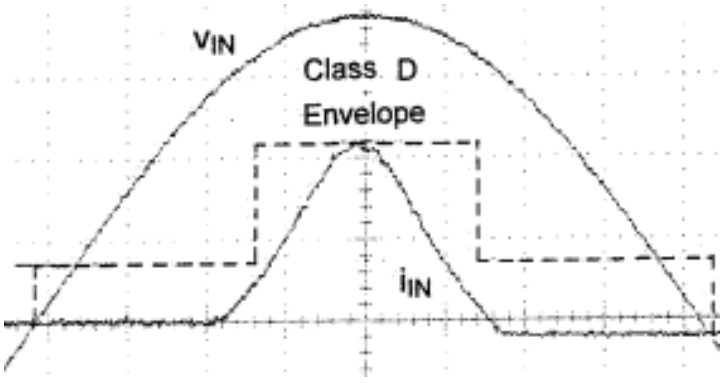

(c)

Figure 1.9: (a) Single-stage flyback converter with magnetic switch. (b) Single-stage flyback converter with counter voltage capacitor. (c) Typical input current waveform for single-stage converters that use a counter voltage (reproduced from [42]).

due to the fact that significant dead-band regions – regions where current is zero – appear around the zero-crossing regions of the input line current. These dead-bands are the result of voltage appearing at the output of the diode bridge rectifier as a result of the counter voltage that is applied. When the input voltage is near zero, the diodes of the bridge rectifier are reverse-biased so that they cannot conduct. It is only after the amplitude of the input voltage exceeds that of the counter voltage that these diodes can conduct.

The result of the input current distortion is higher harmonic content and lower input power factor. The higher harmonic content increases current stress on the converter components, and also reduce converter efficiency. Another negative effect of the increase harmonic content is that they limit the load range over which these converters can operate. Given that the most consideration in the design of AC-DC converters is that their input current meets regulatory agency standards on harmonic content, it becomes increasingly difficult to design a magnetic switch single-stage converter to do so as the load range is increased unless some other performance criteria is compromised, such as efficiency, or component stress.

1.2.4.2 Buck-boost PFC Flyback

Most AC-DC single-stage converters that have been proposed have a boost converter input section. Some researchers have proposed replacing the boost input section with a buck-boost converter section so that the DC bus voltage can be reduced. A buck-boost section is preferred over a buck converter as it is easier to integrate a flyback converter with a buck-boost converter. Several researchers have proposed integrating a flyback converter with a SEPIC converter, which is another topology with voltage step-up / step/down capability.

An integrated buck-boost type flyback converter is shown in Fig. 1.10 [44]. It consists of a buck-boost AC-DC input section and a flyback converter. The converter works as follows: When the switch is ON, capacitor C_{bus} impresses voltage across the transformer as this element is placed across it. Also, snubber capacitor C, which has been charged in the previous switching cycle, quickly discharges through inductor L and the switch. When C has been discharged, the full rectified input voltage is impressed across L and the current through it rises. When the switch is turned OFF, current from L is transferred to C_b through

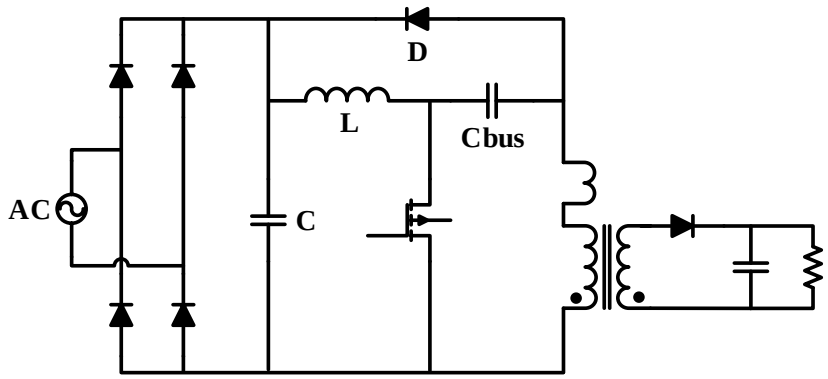

Figure 1.10: Bridgeless Flyback PFC converter.

diode; eventually this current falls to zero before the start of the next switching cycle. Also, leakage inductance energy is transferred to snubber capacitor C and energy that was stored in the transformer previously in the switching cycle is transferred to the output.

The main advantage of single-stage buck-boost converters is that the issue of excessive DC bus is avoided as input voltage, especially high-line input voltage, can be stepped down. As a result, there is no need to distort the input current as is done with some of the other approaches that have been discussed above and thus the converter can operate with an excellent input power factor.

The main drawback is converter efficiency. A buck-boost type converter is not as efficient as a boost-type converter due to its nature. The switches in buck-boost converters have higher turn-off losses as their peak current is higher and this results in a drop in efficiency.

1.2.4.3 Bridgeless Flyback PFC converter

Thus far in this literature review, it has been emphasized that single-stage converters have an uncontrolled DC bus voltage as they are implemented with just a single controller that regulates the output voltage. The DC bus voltage is dependent on the energy equilibrium between energy being transferred to the DC bus capacitor and energy being transferred out of this capacitor. The problem that has been emphasized is the issue of excessive DC bus

voltage – especially if the converter is designed to operate with a universal input line range and it is operating with high input line voltage and light load.

Another issue with single-stage converters, which is the flip side of the excessive DC bus voltage issue, is low efficiency when a universal input range converter is operating with low input line voltage. A universal input range converter design that ensures that the DC bus voltage is not excessive can result in this voltage being very low (i.e. 100 V < V_{bus}< 150 V) when the converter is operating at low input line. When this happens, there is a significant amount of current circulating in the primary side of the converter and this creates significant conduction losses that reduce converter efficiency.

One source of these conduction losses is the conduction loss of the primary side diodes, which can include the input bridge rectifier diodes, the boost section diode (as most converters are boost-derived) and any additional diodes that may be present in the converter's primary side. Primary side current may have to flow through at least three diodes at any given time.

In order to reduce these diode-related conduction losses, so-called bridgeless converters such as the one shown in Fig. 1.11 have been proposed. These converters do not have a diode bridge and rectify the input AC voltage by other means instead, generally by integrating the converter switch with input diodes or replacing bridge diodes with switches that also help perform DC-DC conversion.

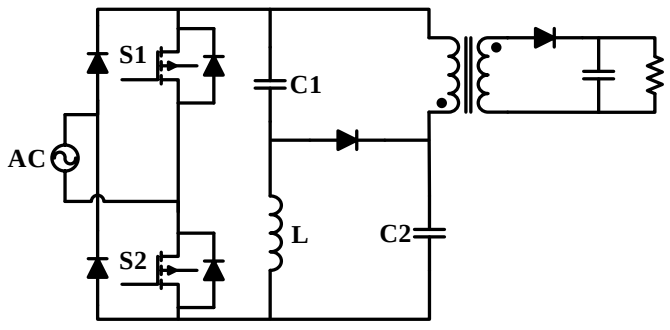

Figure 1.11: Single-stage buck-boost flyback converter.

The converter shown in Fig. 1.11 is a bridgeless AC-DC frond-end combined with a flyback converter with a lossless snubber [46]. The converter operates as follows: The two switches are turned ON and OFF simultaneously. Assuming that the two DC bus capacitors are charged, when the two switches are turned ON, the full AC input voltage is impressed across the input inductor and current rises. While this is happening, the two DC bus capacitor discharge – C_2 discharges through inductor L and C_1 discharges through the transformer. As C_2 impresses voltage across the transformer, energy is stored in it.

When the switches are turned OFF, the input inductor current flows through C_1 and C_2 and falls. Eventually, this current falls to zero and remains at zero until the start of the next switching cycle when the switches are turned on again. In the meantime, energy that was stored in the transformer when the switches were ON is transferred to the output through the secondary diode.

It should be noted that even though the input current flows through three circuit elements at any given time, some reduction in conduction losses can occur if the switches are MOSFET devices with low on-stage resistance values (R_{ds-on}). With such MOSFETs, conduction losses are lower than those produced by diodes with much higher forward voltage drops.

Although bridgeless single-stage converters can be more efficient than single-stage converters with input diode bridges, especially at low input line, they have several drawbacks, including the following:

- The lack of an input bridge has little, if any, impact on the DC voltage so that the issue of excessive DC bus voltage remains unless some DC bus voltage reduction method such as the ones discussed in this thesis are implemented.
- Converter cost and complexity can increase if the bridgeless converter requires additional active devices such as the converter shown in Fig. 1.11.
- Some bridgeless converters have issues with EMI as their topologies do not allow for stable grounding [48]. This results in additional EMI filtering being needed so that the converter size is increased.

1.3 Thesis Objectives

The main objectives of this thesis are presented as follows:

- To propose a new two-switch single-stage AC-DC flyback converter with double power transfer frequency and low peak voltage stress by using only one active clamp switch.
- To analyze the proposed converter in order to study its steady state characteristics.
- To develop a circuit design procedure for the new single-stage converter that can be used in the selection of circuit components.
- To confirm the feasibility of the new single-stage converter with experimental results obtained from a 200W prototype converter.

1.4 Thesis outline

This thesis consists of six chapters. The outline of the thesis is as follows:

In Chapter 2, a new single-phase single-stage AC-DC stacked flyback converter with only one active clamp switch is proposed. The stacked converter concept is introduced and its modes of operation is presented. The converter features are listed to demonstrate the advantages of the proposed converter.

In Chapter 3, a steady-state analysis of the proposed converter is performed. Each key mode of operation is analyzed in detail using mathematical equations derived for that mode. A computer program is developed and used to find potential operation points of the converter over an input voltage and output load range on the principle of energy equilibrium. Graphs of design curves of key parameters generated by this computer program are also presented.

In Chapter 4, the design of the proposed converter is presented. The design is mainly based on computer program and design curves presented in the previous chapter. Key parameters

of the proposed converter are determined based on the converter analysis. The design procedure is demonstrated with a design example for a particular set of specifications.

In Chapter 5, experimental results are presented. The experimental results use the specifications as those of the design example in the previous chapter. The experimental results are obtained from a 200W prototype converter. The feasibility of the proposed converter is confirmed and the efficiency of the proposed converter is presented.

In Chapter 6, a summary of the thesis is presented along with conclusions, contributions and possible future work that can be performed.

Chapter 2

2 AC-DC Single-Stage Stacked Flyback Converter

2.1 Introduction

The proposed AC-DC single-stage converter is introduced in this chapter. The converter is based on the concept of stacking single-stage converter modules on top of each other. In this chapter, the general operation and the modes operation of proposed converter are explained, the features of the proposed converter are stated and the extension of the stacked converter concept to other single-stage converter modules is discussed.

2.2 Converter concept

The proposed converter is shown in Fig. 2.1. It is made up of two flyback converters that are stacked on top of each other at the primary and connected in parallel at the output, an active clamp auxiliary circuit that is used to help the main power switches turn on with zero-voltage switching (ZVS) and a front-end AC-DC boost section that consists of a diode

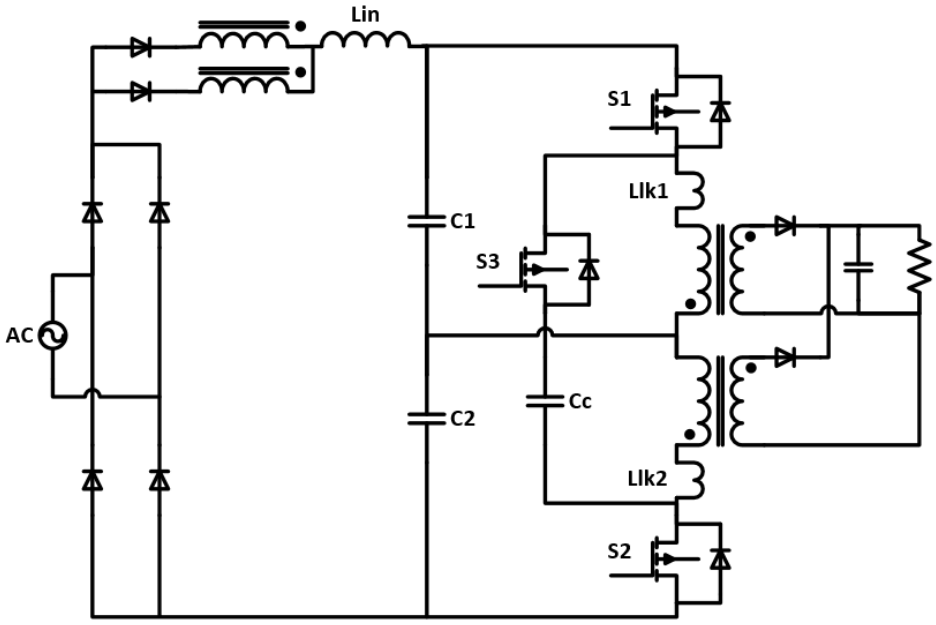

Figure 2.1: Single-stage single-phase AC-DC stacked flyback converter.

bridge, an input inductor L_{in} and two auxiliary windings that are each taken from one of the flyback transformers and that are each connected in series with a blocking diode. Inductances L_{lk1} and L_{lk2} may be a combination of the transformer leakage inductances and some external inductances or just the leakage inductances. L_{lk1} and L_{lk2} help in the ZVS operation of the converter by storing energy that can be later used to discharge the switch output capacitances before turn-on.

The auxiliary windings act as 'magnetic switches' that cancel the DC bus capacitor voltage so that the voltage that appears at the right-hand side of input inductor L_{in} is zero. When the upper switch S_1 is on, the primary voltage of the main transformer T_1 is positive, auxiliary winding (N_{aux1}/N_1=2) that cancels out the DC bus voltage so that the currents in input inductors L_{in} rise. When the lower switch S_2 is on, the primary voltage of the main transformer is negative, auxiliary winding (N_{aux2}/N_1=2) cancels out the DC bus voltage so that the currents in input inductors L_{in} rise. When there is no voltage across the main transformer primary winding, the total voltage across the DC bus capacitors appears at the output of the diode bridges and the input currents fall since this voltage is greater than the input voltage. If the input current is discontinuous, it has a sinusoidal envelope and is in phase with the input voltage.

2.3 Modes of operation

Typical converter waveforms are shown in Fig. 2.2 and equivalent circuit diagrams that show the converter's modes of operation are shown in Fig. 2.3 with the diode bridge output replaced by a rectified sinusoidal voltage source. The converter has the following modes of operation during an entire switching cycle.

Mode 1 ($t_0 < t < t_1$): *(Fig. 2.3(a))*

In this mode, switch S_1 is ON and the energy is stored in the transformer T_1. At the same time, since S_2 is OFF, stored energy in the magnetizing inductance of transformer T_2 is transferred to the load. Since the auxiliary winding generates a voltage that is equal to the total DC bus voltage with opposite polarity, which cancels the total DC bus capacitor

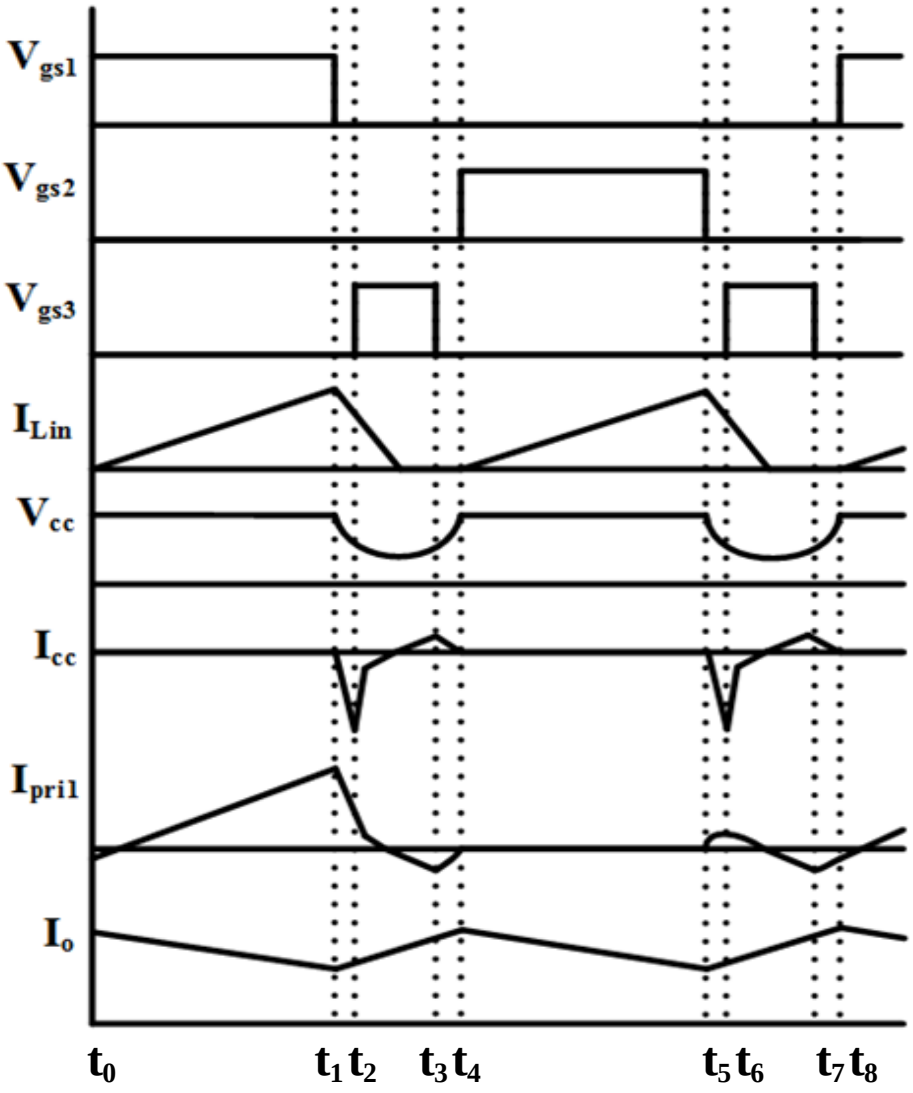

Figure 2.2: Typical waveforms of proposed converter for upper flyback converter.

voltage, the voltage across the input inductor is the rectified supply voltage; thus the input current in L_{in} rises.

Mode 2 ($t_1 < t < t_2$): *(Fig. 2.3(b))*

In this mode, S_1 is OFF. The only path for the stored energy in the leakage inductance of T_1 to flow is through capacitor C_c and the body diode of the active clamp switch S_3, through the lower bus capacitor C_2 and the output capacitor of S_2.

Mode 3 ($t_2 < t < t_3$): *(Fig. 2.3(c))*

In Mode 3, the auxiliary switch S_3 is turned ON to start this mode. The stored energy in capacitor C_c flows through the leakage inductor L_{lk2}, the primary winding of the transformer T_2, the primary winding of transformer T_1, the inductor L_{lk1}, and auxiliary switch S_3. Since the output diode is ON during this mode, there is no energy stored in transformer T_1.

Mode 4 ($t_3 < t < t_4$): *(Fig. 2.3(d))*

In this mode, switch S_3 is OFF. Current in the leakage inductance of T_2, L_{lk2}, flows through the output capacitor of S_2 and bulk capacitor C_2. It discharges the output capacitor of S_2 so that S_2 can be turned on with ZVS. This also happens for S_1 and the output capacitor of S_1 discharges in Mode 8. Since S_1 is not turned ON, its output capacitor is eventually fully recharged.

Mode 5($t_4 < t < t_5$): *(Fig. 2.3(e))*

In this mode, switch S_2 is ON with ZVS. The primary current flows through the magnetizing inductance of T_2 and increases while the stored energy in the magnetizing inductance of T_1 is transferred to the load through the secondary diode.

Mode 6 ($t_5 < t < t_6$): *(Fig. 2.3(f))*

In this mode, switch S_2 is OFF. The only path for the stored energy in leakage inductance L_{lk2} is to flow through capacitor C_c and the body diode of the active clamp switch S_3 through the lower bus capacitor C_1 and the output capacitor of S_2.

Mode 7 ($t_6 < t < t_7$): *(Fig. 2.3(g))*

The auxiliary switch S_3 is turned ON at the start the mode. The stored energy in capacitor C_c flows through the leakage inductor L_{lk2}, the primary winding of the transformer T_2, the primary winding of transformer T_1, the inductor L_{lk1}, and auxiliary switch S_3. Since the output diode is ON during this mode, there is no energy stored in transformer T_2.

Mode 8 ($t_7 < t < t_8$): *(Fig. 2.3(h))*

In this mode, auxiliary switch S_3 is OFF. Current in inductor L_{lk1} flows through the output capacitor of S_1 and bulk capacitor C_1. It discharges the output capacitor of S_1 so that S_1 can

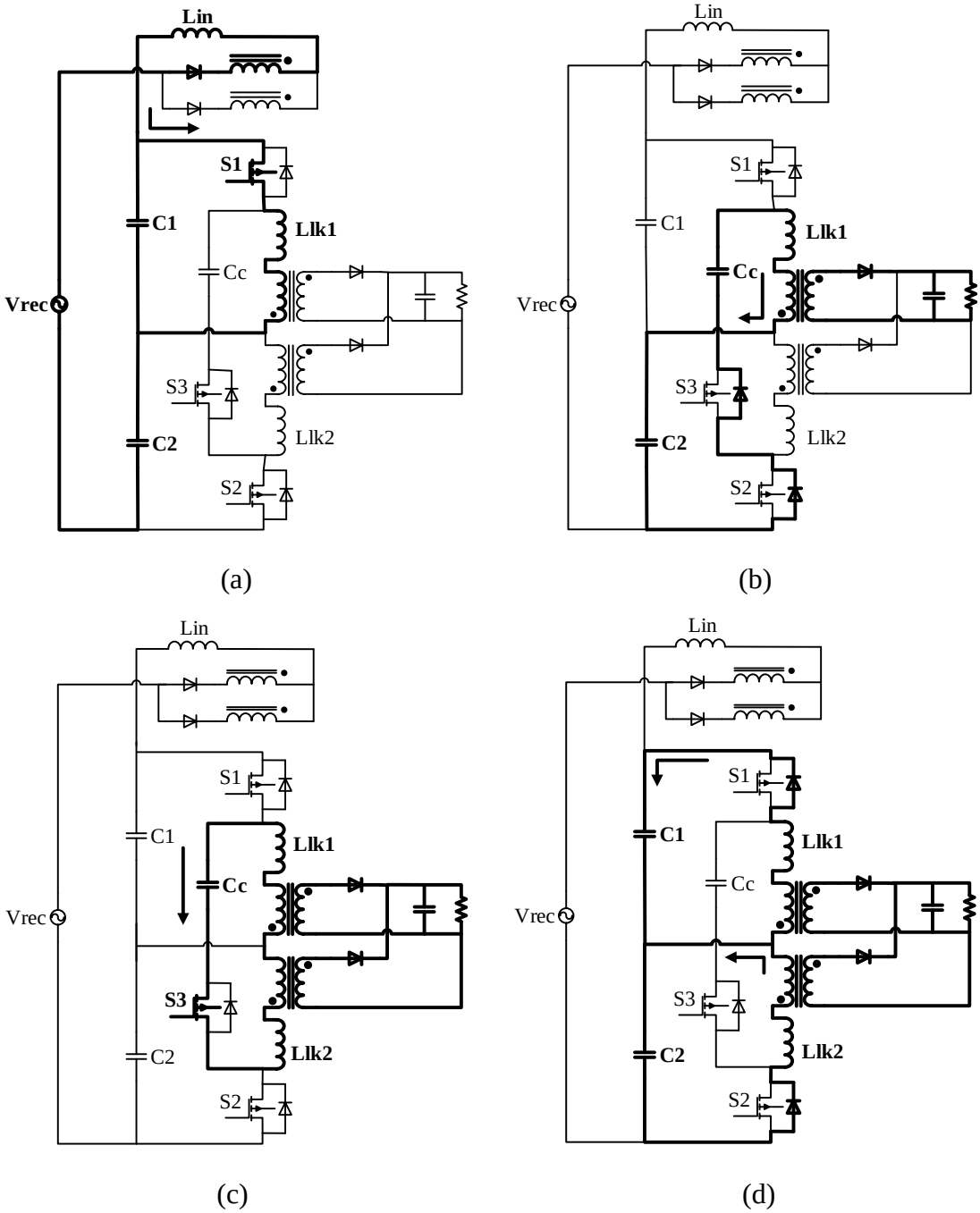

Figure 2.3: Modes of operations

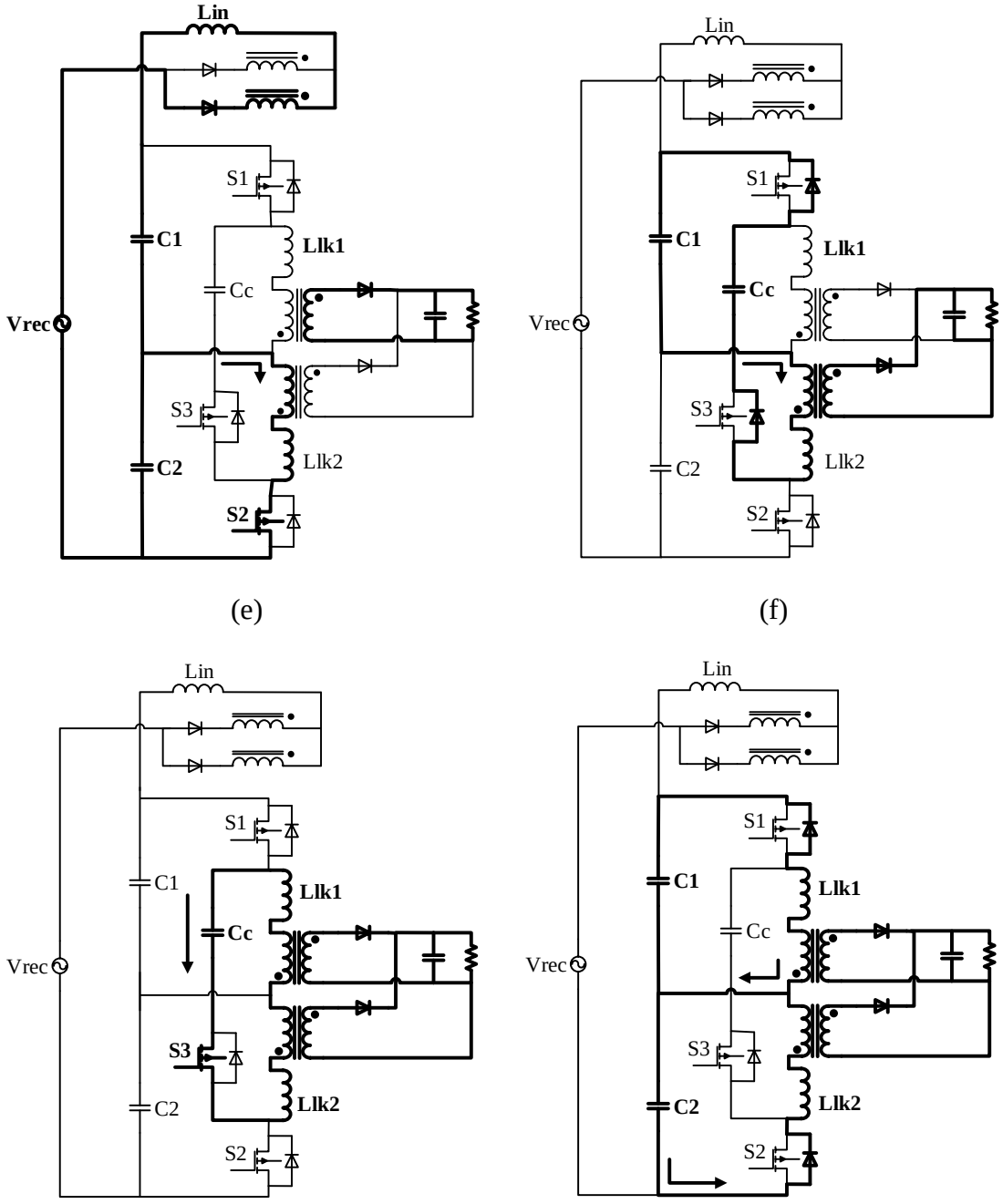

Fig 2.3 (*continued*)

be turned ON with ZVS. Since S_1 is not turned ON, its output capacitor is eventually fully recharged.

2.4 Converter feature

The proposed converter has the following features:

- Exposure to excessive DC bus voltages by converter components is avoided due to the stacked topology. The converter components on the primary side (i.e. switches) are exposed to just half the DC bus voltage.
- Since excessive DC bus voltages are less of a concern than with conventional, non-stacked single-stage converters, there is greater flexibility in the design of the converter. Most notably, the input current conduction angle does not have to be limited so that input current distortion is reduced and input power factor is increased.
- Both converter switches can operate with soft-switching using a single active auxiliary switch instead of having to use two auxiliary switches – one for each switch.
- The converter can operate with greater light-load efficiency since CV^2 losses are reduced as the converter switches are exposed to only half the DC bus voltage. Most converters with auxiliary circuits for ZVS operation are either ineffective when the converter is operating with light loads or create more losses than they save under these conditions. The proposed converter has superior light-load efficiency.
- Power transfer can occur throughout the switching period as opposed to being limited to around 50% maximum because the converter has two switches instead of one. In conventional single-stage flyback converters, operating with a duty-cycle above 50% means that peak voltage stress of the single switch must be increased considerably or the converter must operate with small duty cycles at high-line voltages. For the proposed converter, the peak voltage stress in the switches is much less because switch duty cycles > 50% are avoided; this reduction is on top of the voltage stress reduction due to the stacked topology. In other words, two lower power rated, cheaper and more widely available devices can be used instead of a very expensive single device.

2.5 Other Implementations of the Stacked Concept

The proposed converter is just one way of implementing the stacked converter concept. In general, it can be implemented with any single single-stage converter module that has auxiliary windings from the main transformer. The basic idea is to stack one module on

top of the other as shown in Fig. 2.4, then connect the auxiliary windings appropriately at the input and interleave the output windings as in Fig. 1.7(a). How this can be accomplished will be explained as follows in this section of the thesis. Much of the following discussion is taken from [10].

Although many single-stage AC-DC flyback converters, which are referred to as input current shapers (ICSs) in [10], have been proposed, these converters share a number of common properties. A number of ICSs can be classified as being two-terminal ICSs and three-terminal ICSs, as shown in Fig. 2.5 and Fig. 2.6. Two-terminal ICSs operate based on the principle of the 'magnetic switch' must like the module converters in the proposed converter. The basic structure of a two-terminal ICS is shown in Fig. 2.7(a), where it can be seen that the ICS has a discharge branch and a charge branch and that the two branches are in parallel. The input inductor current is made to rise by 'charging' the inductor through the charge branch and is made to fall by allowing current to flow into the 'discharge' branch. In the proposed converter, which uses two-terminal ICS modules, current flowing through the charge branch corresponds to Mode 1 of operation and current flowing through the discharge branch corresponds to Mode 5 of operation.

Three-terminal ICSs also have discharge and charge branches, but the charge branch is not connected in parallel to the discharge branch. This branch is, instead connected to the input switch as shown in Fig. 2.7(b). The proposed converter can be implemented with two-terminal ICSs, but not with three-terminal ICSs because only modules with magnetic switches can be used. It is, however, possible to convert a three-terminal ICS into a two-terminal ICS, as explained in [10].

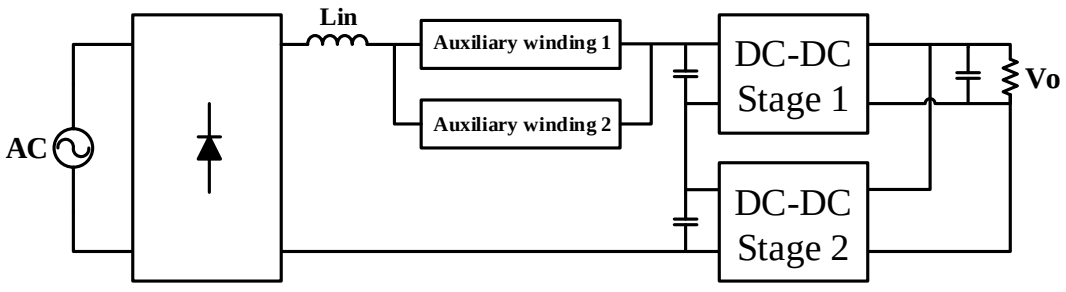

Figure 2.4: Modular diagram of proposed stacked single-stage converter concept.

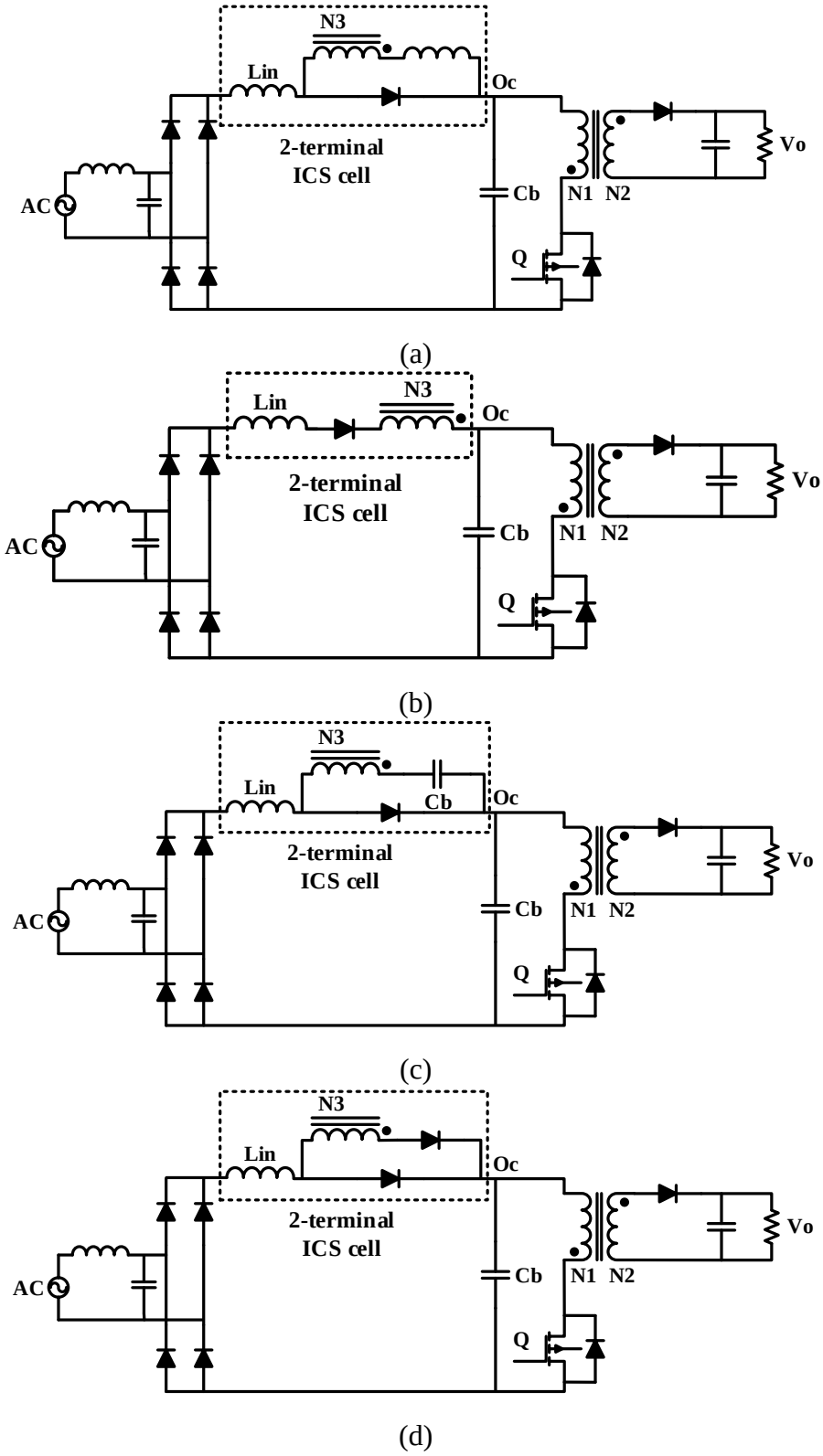

Figure 2.5: Example single-stage converters with two-terminal input current shaper (ICS) cells [10].

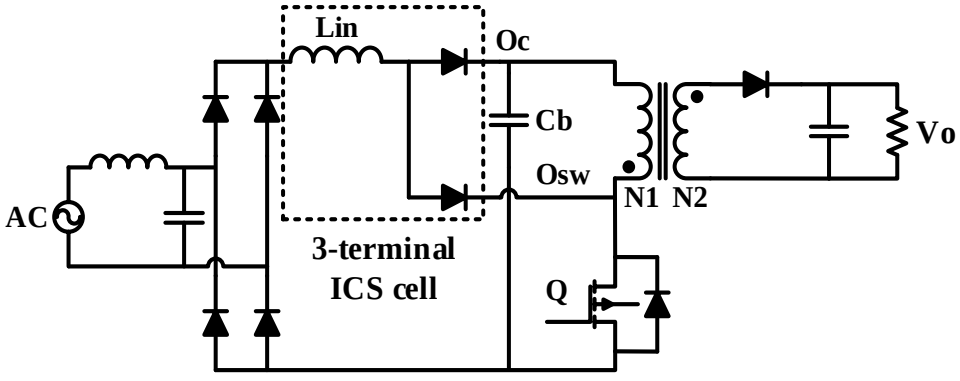

(a)

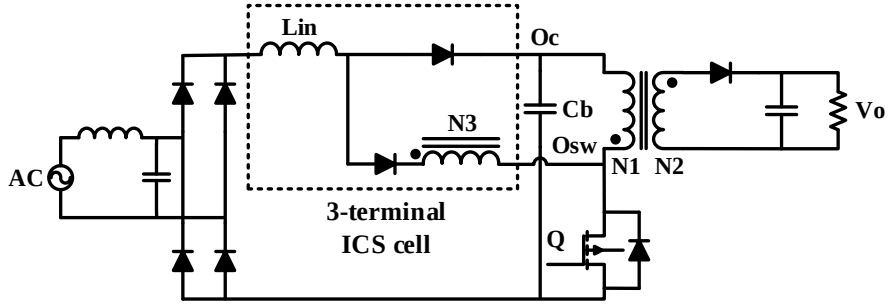

(b)

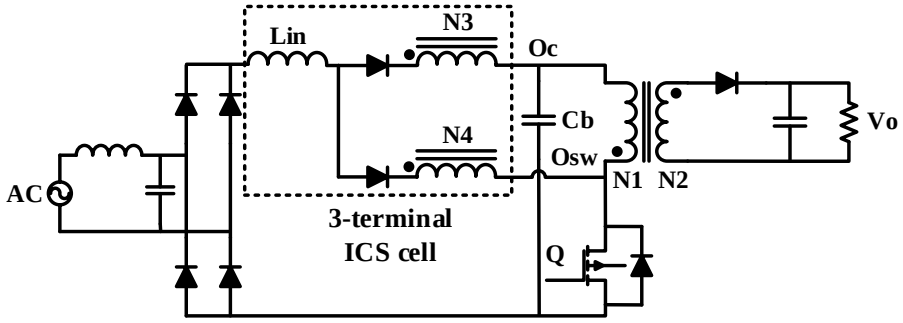

(c)

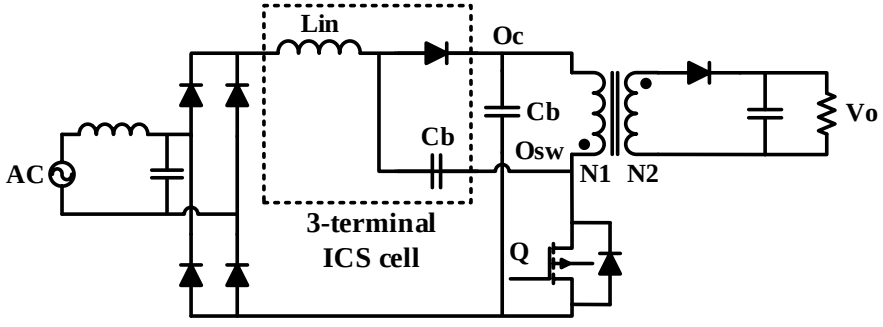

(d)

Figure 2.6: Example single-stage converters with three-terminal input current shaper (ICS) cells [10].

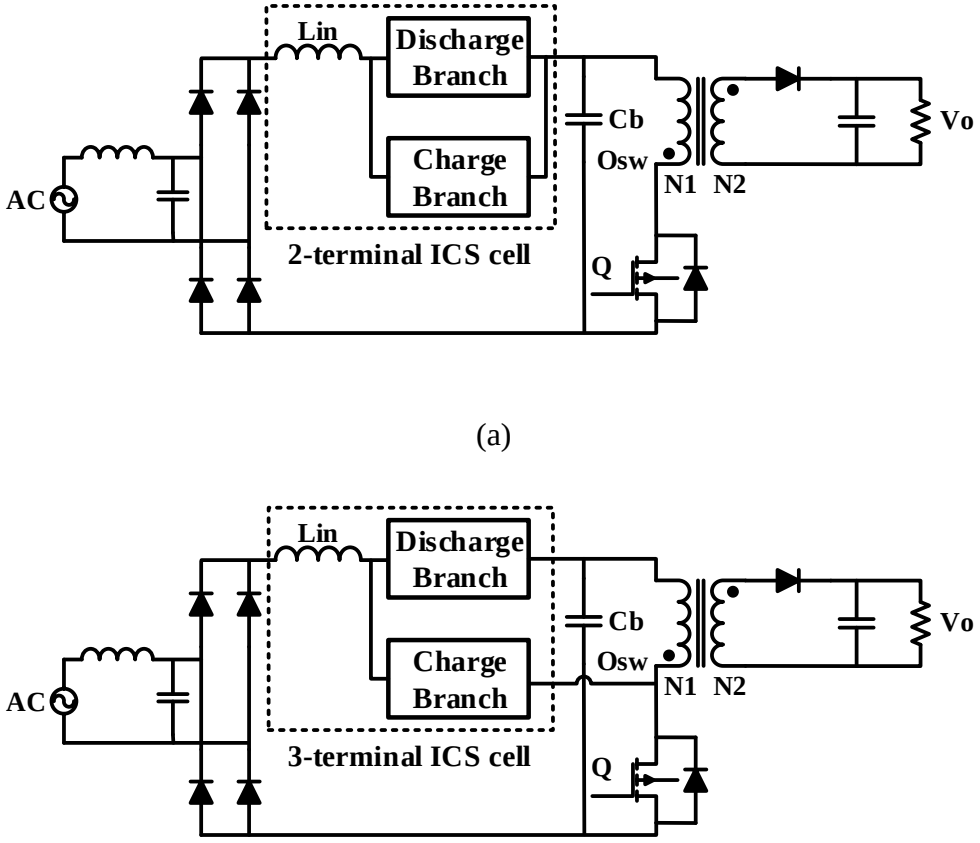

Figure 2.7: Single-stage PFC with generic ICS cell (a) two-terminal (b) three-terminal [10].

The general rule is to take a three-terminal ICS cell and add an extra winding as shown in Fig. 2.8(a). The polarity of the added winding should be such that the equivalent circuit before and after the translation is the same when the switch is on, as shown in Fig. 2.8(b). The number of turns of the added winding should equal that of primary winding of the transformer in the DC-DC converter section if the original three-terminal ICS charge branch had a direct connection to the main converter switch. If the connection is through an auxiliary winding that produces a counter voltage to change the energy equilibrium at the DC bus to a more favorable one like the converter shown in Fig. 2.9 [42], then the number of turns of the added winding should be such that the counter voltage is reproduced

when the switch is turned on. It should be noted that the discharge branch remains same before or after translation from three-terminal ICS to two-terminal ICS.

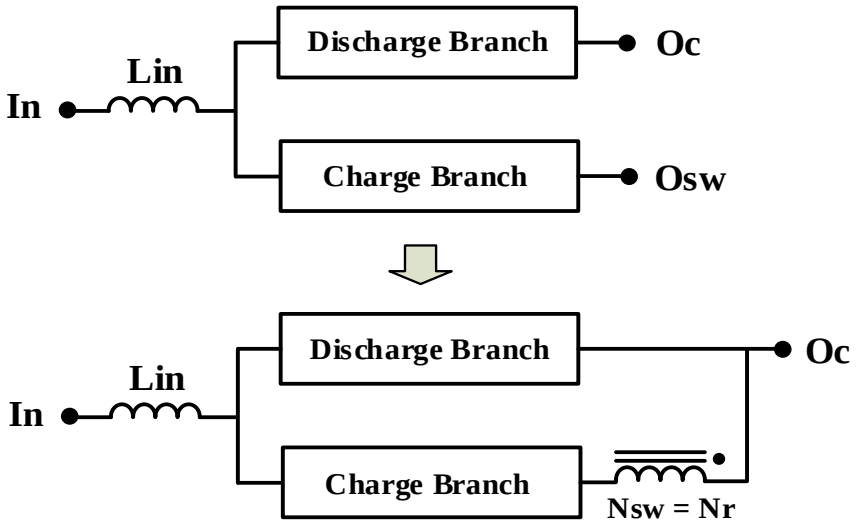

(a)

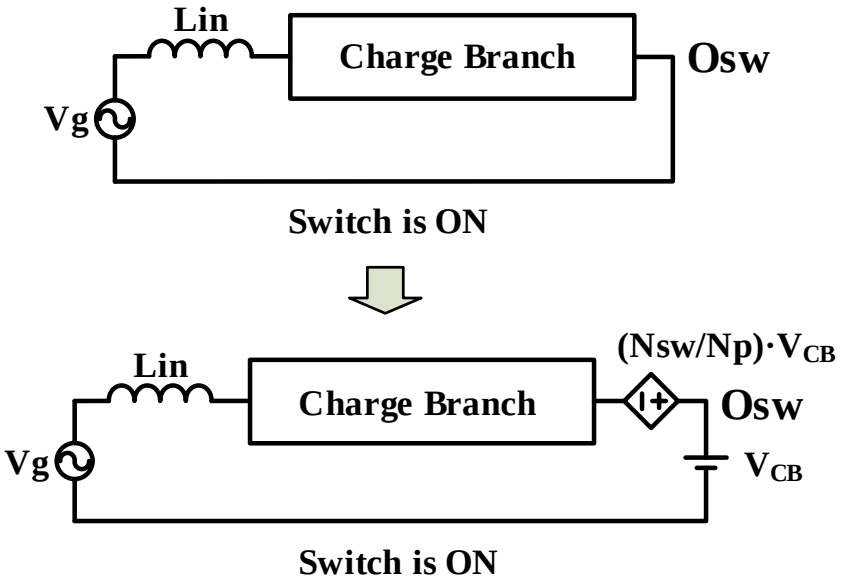

(b)

Figure 2.8: Translation from three-terminal ICS cell to two-terminal ICS cell. (a) Adding one additional winding. (b) Equivalent circuit when switch is on.

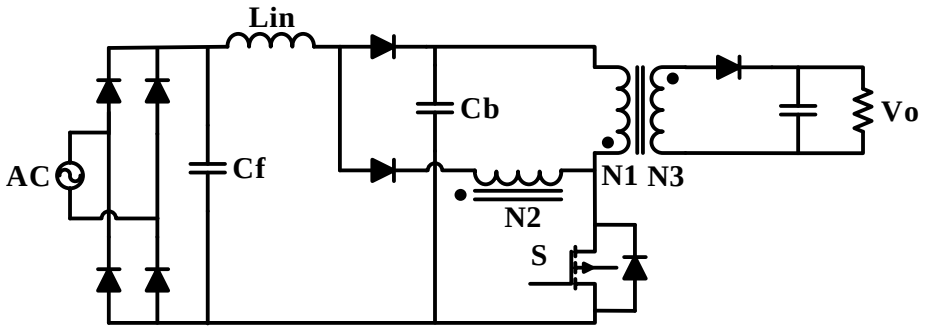

Figure 2.9: AC-DC single-stage converter with auxiliary winding that produces counter voltage proposed in [42].

2.6 Conclusion

The proposed AC-DC single-stage converter was introduced in this chapter. In this chapter, the general operation and the modes of proposed converter were explained and its features were stated. Since the converter's topology was based on the stacking of single-stage converter modules on top of each other, the extension of the stacked converter concepts to other single-stage converter modules was discussed. In order for a single-stage converter to be implemented as a module in a stacked converter, it must have a magnetic switch. Such a switch is implemented using an auxiliary winding from the main transformer. It was shown in this chapter that numerous, previously proposed single-stage converters, whether they be two-terminal input current shapers or three-terminal input current shapers, can be stacked as long as they have magnetic switches or have equivalent topologies with magnetic switches.

Chapter 3

3 Circuit Analysis

3.1 Introduction

In the previous chapter, the general operation and the key modes of operation of the proposed converter were explained. The steady-state characteristics of key converter parameters are determined by a mathematical analysis of the converter's modes of operation in this chapter. In this chapter, mathematical equations that define each mode of the proposed converter are derived and these equations form the basis of a computer program that will allow graphs of characteristic curves to be plotted. These graphs will then be used in the next chapter to develop a procedure for the design of the proposed converter.

3.2 Circuit Steady-state analysis

For the steady-state analysis of the proposed converter's modes of operation, the following assumptions have been made:

- The auxiliary winding turns ratio is 2:1 in order to cancel the entire DC bus voltage. This allows each converter modules to emulate a single-stage converter with no counter voltage applied to its input inductor. This counter voltage reduces the amount of energy stored in the input inductor and affects the energy equilibrium at the DC bus.
- All semiconductors do not have voltage drops when they are turned ON.
- The output capacitor is sufficiently large so that it has no voltage ripple.
- The upper and lower converter modules of the proposed converter are identical (the DC bus capacitor C_1 and C_2 are the same, the switches, semiconductors, transformer ratings are the same).

The objective of the steady-state analysis is to obtain the current that goes in and goes out of the intermediate DC bus capacitor. As mentioned in previous chapters, single-stage AC-DC converters do not have control of the DC bus voltage because they only have one controller to regulate the output voltage. Under steady-state conditions, the average current

flowing into the DC bus from the input should be equal to the average current flowing out of the DC bus to the output so that energy equilibrium is achieved at the DC bus. By considering this DC bus equilibrium for a particular set of line, load and converter parameters, the duty cycle of the converter (ratio of switch on-time to period) can be determined and the voltages and currents of the converter components can be determined. If this process is implemented in a computer program and repeated numerous times, then graphs of steady-state characteristic curves that give a clearer picture of how the converter operates can be determined. The computer program and design curves will be presented in following sections below.

The first step of the analysis is to determine equations that define the operation of the proposed converter during each mode of operation. This can be done as follows:

Mode 1 ($t_0 < t < t_1$): *(Fig. 3.1)*

The equivalent circuit of Mode 1 is shown in Fig. 3.1. Based on the assumption made previously, an auxiliary winding T_3 turns ratio 2:1 generates a voltage that is equal to the

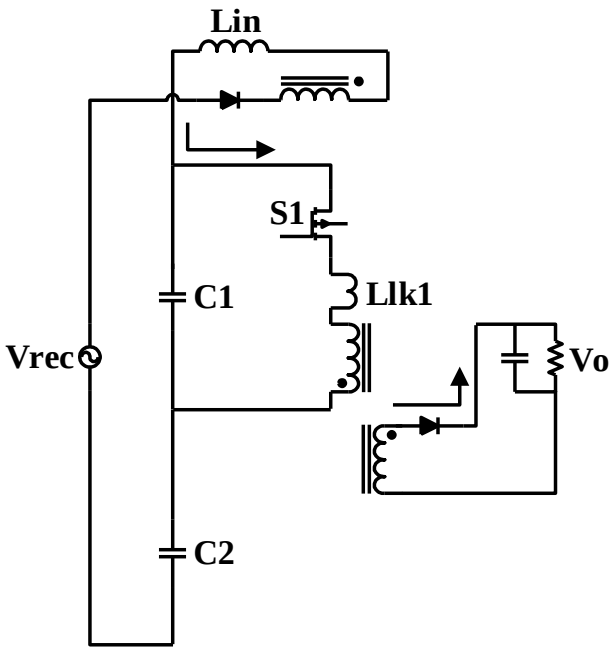

Figure 3.1: Equivalent circuit of Mode 1.

total DC bus voltage, but with opposite polarity. The input voltage across the input inductor is thus the rectified supply voltage so that input current in L_{in} rises according to

$$i_{Lin,k}(t) = \frac{|v_{in,k}| \cdot t}{L_{in}} \tag{3.1}$$

where $|v_{in,k}|$ is the rectified AC input voltage during switching cycle interval *k*. The input voltage can be considered to be a constant value in a single switching cycle as the switching frequency is much higher compared with the AC input line frequency. The current in the input inductor L_{in} at the end of Mode 1 is

$$i_{Lin,k,sum1}(t) = \frac{|v_{in,k}|}{L_{in}} \cdot \frac{D}{2f_{sw}} \tag{3.2}$$

Duty cycle D is defined as the time when main switch S_1 or S_2 is ON during the entire switching cycle (two switches are ON for exactly the same length of time but in alternative half cycles). The two switches are each operated in during an alternative half switching cycle $T_{sw}/2$ or $2f_{sw}$ where f_{sw} is the switching frequency of the main switch.

Mode 2 (t_0 < t < t_1): *(Fig. 3.2)*

The equivalent circuit of Mode 2 is shown in Fig. 3.2. Because there is no switch closed during this mode, the current in the circuit is circulating and energy in the leakage

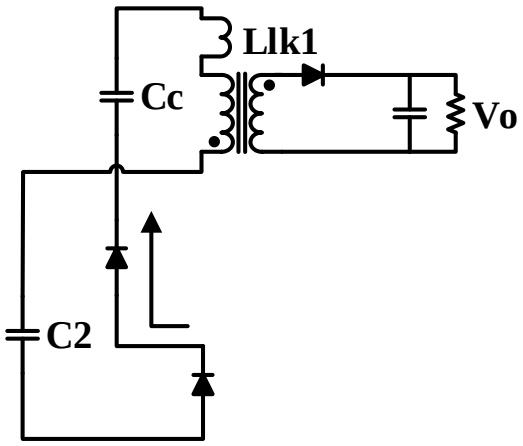

Figure 3.2: Equivalent circuit of Mode 2.

inductance flows though the active clamp capacitor. Following Kirchhoff's Voltage Law (KVL), the following equation can be established:

$$\frac{V_{bus}}{2} + (L_{lk1} + L_{m1})\frac{di}{dt} = V_{clamp} \tag{3.3}$$

where the two bus capacitors equally divide the DC bus voltage. L_{lk1} is the leakage inductance of the upper converter transformer while L_{m1} is the magnetizing inductance of upper converter transformer. V_{clamp} is the voltage across the clamp capacitor. During this mode, the energy in main transformer T_1 is transferred to the output load until the current in the transformer goes zero. The output voltage can be expressed as follows:

$$L_{m1}\frac{di}{dt} = Nv_0 \tag{3.4}$$

where N is the transformer turns ratio between the primary and secondary (N_1/N_2).

Mode 3 (t_0 < t < t_1): *(Fig. 3.3)*

The equivalent circuit of Mode 3 is shown in Fig. 3.3. Auxiliary switch S_3 is turned ON with ZVS. The energy in transformer T_1 is transferred to the output load while the energy in clamp capacitor is transferred to leakage inductor $L_{lk2,}$ according to

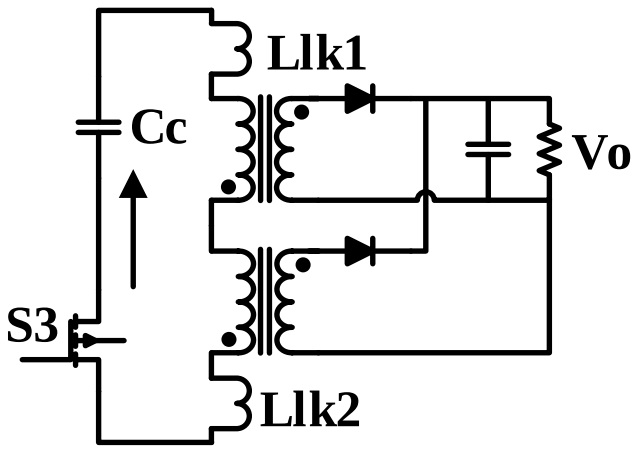

Figure 3.3: Equivalent circuit of Mode 3.

$$(L_{lk1}+L_{lk2} + L_{m1} + L_{m2})\frac{di}{dt} = V_{clamp} \quad (3.5)$$

Mode 4 ($t_0 < t < t_1$): *(Fig. 3.4)*

The equivalent circuit of Mode 4 is shown in Fig. 3.4. This mode starts when the active clamp switch S_3 is OFF. Current in leakage inductance L_{lk2} flows through the output capacitor of S_2 and C_2 according to

$$\frac{V_{bus}}{2} + (L_{lk2} + L_{m1})\frac{di}{dt} = V_{clamp} \quad (3.6)$$

This output capacitor is discharged so that S_2 can be turned ON with ZVS.

Mode 5 ($t_0 < t < t_1$): *(Fig. 3.5)*

The equivalent circuit of Mode 5 is shown in Fig. 3.5. This mode starts the operation of lower converter. The lower transformer T_2 generates a counter voltage to cancel the DC

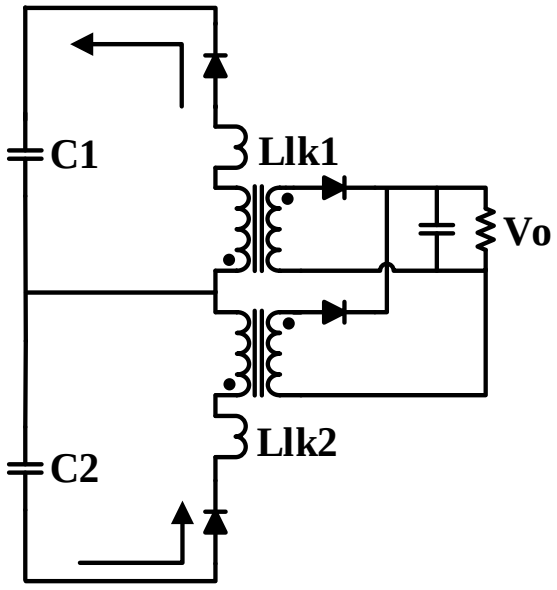

Figure 3.4: Equivalent circuit of Mode 4.

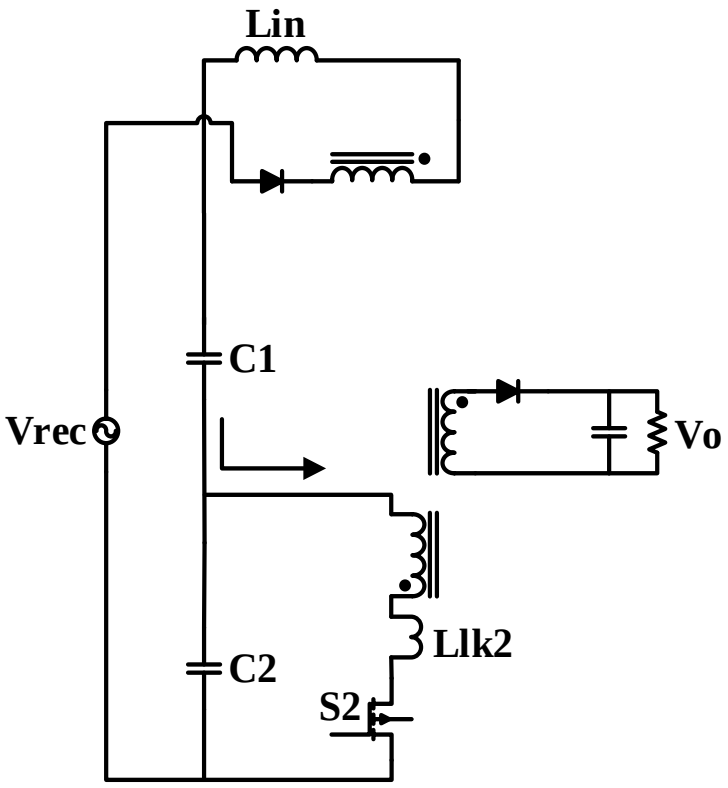

Figure 3.5: Equivalent circuit of Mode 5

bus voltage. As the converter specification is exactly the same, the current in the input inductor in Mode 5 in the second part of the switching cycle is same in Mode 1 according to

$$i_{Lin,k,sum2}(t) = \frac{|v_{in,k}|}{L_{in}} \cdot \frac{D}{2f_{sw}} \tag{3.7}$$

The current is bounded by a sinusoidal envelope related to the input rectifier voltage, as shown in Fig. 3.6, and it rises and falls twice in one switching cycle f_{sw}. The ON time for each switch is

$$T_{on} = D \cdot T_{sw} \tag{3.8}$$

so that the total input current in interval k is

$$i_{Lin,k} = \frac{|v_{in,k}|}{L_{in}} \cdot \frac{D^2}{4{f_{sw}}^2} \tag{3.9}$$

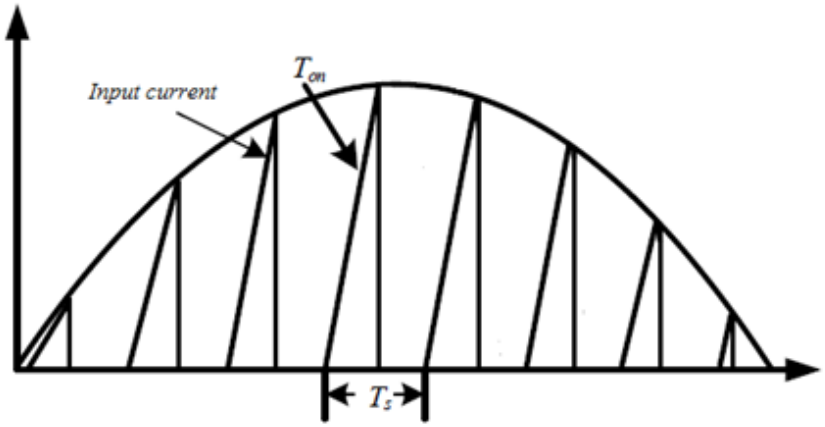

Figure 3.6: DCM operation on input inductor.

The input inductor current flows into the DC bus capacitor as it is the only path that is available to it; therefore, the average current of the input current is the same current injected into the DC bus. By accumulating all the switching intervals together, the average current flowing into the DC bus during AC line cycle is

$$I_{bus,in-avg} = f_{ac} \cdot \sum_{k=0}^{n} \frac{D^2 v_{rec}}{4{f_{sw}}^2 L_{in}} \tag{3.10}$$

where f_{ac} the frequency of AC is input line and n is the number of interval in one AC line cycle

$$n = \frac{f_{sw}}{f_{ac}} \tag{3.11}$$

v_{rec} is the rectified voltage output from the rectified diode bridge that can be determined as follows

$$v_{rec} = V_{rms} \cdot |\sin(2\pi k/n)| \tag{3.12}$$

Equ. (3.10) will eventually be compared to the average current flowing out of the DC bus to determine whether an energy equilibrium has been established and the converter is operating in steady-state.

Mode 6 ($t_0 < t < t_1$): *(Fig. 3.7)*

The equivalent circuit of Mode 6 is shown in Fig. 3.7. This mode is the same as Mode 2 except that the current is flowing through the output capacitor S_3 in order to have zero-voltage across the switch before it is turned on.

Mode 7 ($t_0 < t < t_1$): *(Fig. 3.8)*

The equivalent circuit of Mode 7 is shown in Fig. 3.8. This mode is as the same as Mode 3 except that energy in transformer T_2 continues being transferring to the load.

Mode 8 ($t_0 < t < t_1$): *(Fig. 3.9)*

The equivalent circuit of Mode 8 is shown in Fig. 3.9. This mode is the same as Mode 4. Current flows through the body diode of main switch S_2as shown in the figure.

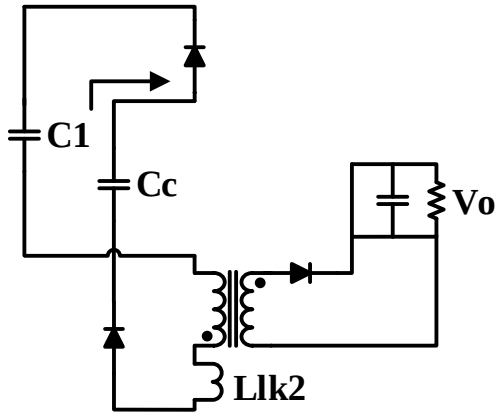

Figure 3.7: Equivalent circuit of Mode 6

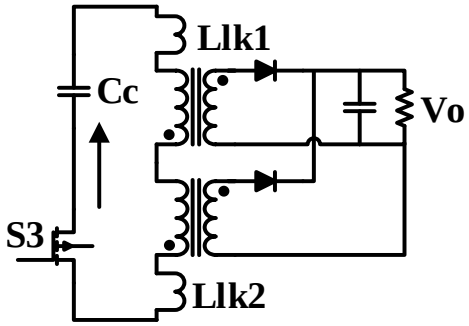

Figure 3.8: Equivalent circuit of Mode 7

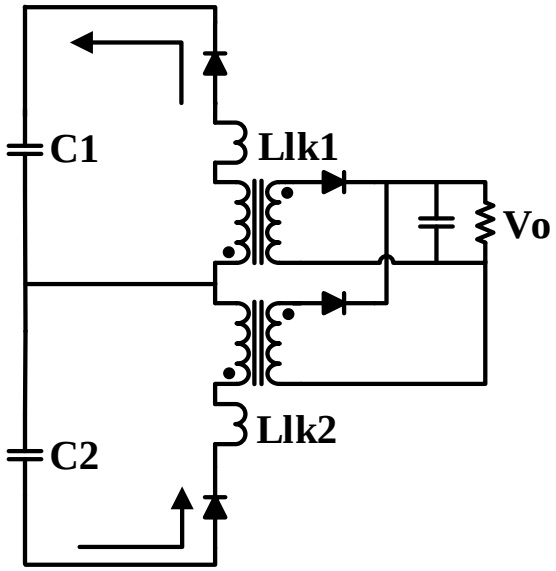

Figure 3.9: Equivalent circuit of Mode 8

3.2.1 Energy equilibrium and the DC bus voltage

The key parameter of the AC-DC single-stage converter that must be derived from mathematic equations is the DC bus voltage because a single-stage converter does not have control of the DC bus voltage as two-stage converters do. According to the theory of energy equilibrium, the energy pumped into the DC bus from the AC-DC section must be equal to the energy transferred to the output so that the net average DC current flowing in and out of the DC bus capacitor must be zero during a half switching cycle. This energy equilibrium, however, cannot be determined using equations with closed-form solutions because the duty cycle is determined by the input source and output load. The only way to determine the duty cycle is by using a computer program. This computer program is based on the assumption that the converter has ideal semiconductors and an ideal transformer with no leakage inductance and negligible magnetizing current. Under these conditions, the DC bus voltage can be determined for any operating point by using the following parameters: input voltage $V_{in,}$ output voltage $V_{o,}$ output current $I_{o,}$ switching frequency $f_{sw,}$

input inductor L_{in} transformer inductor $L_{m,}$ and transformer turns ratio *N*. The procedure to determine the energy equilibrium is shown in the flowchart in Fig. 3.10 and is as follows:

1) Assume a duty cycle D as an initial 'guess' (i.e., D=0.5)
2) Assume that the input inductor current is continuous

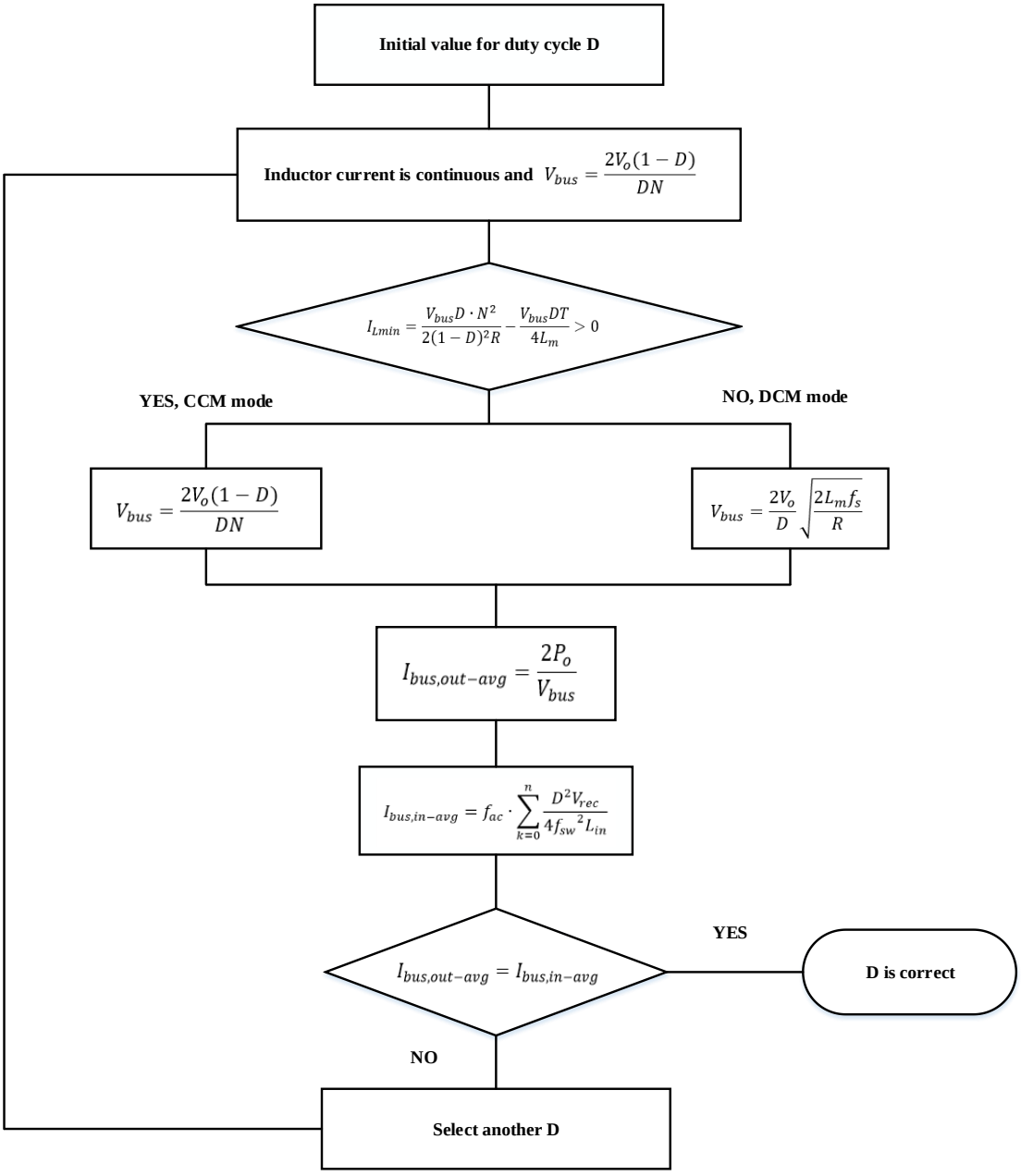

Figure 3.10: The procedure of steady state analysis for determining the DC bus voltage and switching duty cycle.

$$V_{bus} = \frac{2V_o(1-D)}{DN} \tag{3.13}$$

With this value of V_{bus}, the next step is to determine whether the converter operates in continuous mode or discontinuous mode. The criteria is to examine whether the minimum value of input inductor current I_L is larger than zero

$$I_{Lmin} = \frac{V_{bus}D \cdot N^2}{2(1-D)^2R} - \frac{V_{bus}DT}{4L_m} > 0 \tag{3.14}$$

If I_{Lmin} is larger than zero, the input inductor current is continuous, then the value of V_{bus} is equal to $\frac{2V_o(1-D)}{DN}$. If not, the input inductor current is discontinuous, then the value of V_{bus} can be derived from the following equation related to DCM operation:

$$V_{bus} = \frac{2V_o}{D}\sqrt{\frac{2L_m f_s}{R}} \tag{3.15}$$

With the value of V_{bus} known, find the average current flowing out of the DC bus by using the output power and the known bus voltage

$$I_{bus,out-avg} = \frac{2P_o}{V_{bus}} \tag{3.16}$$

then determine the average current that is fed from the AC line to the DC bus

$$I_{bus,in-avg} = f_{ac} \cdot \sum_{k=0}^{n} \frac{D^2 v_{rec}}{4{f_{sw}}^2 L_{in}} \tag{3.17}$$

As mentioned previously, an energy equilibrium must exist for the DC bus capacitors when the converter is operating under steady-state condition; therefore, the next step of the procedure in the computer program is to verify whether $I_{bus,out-avg}$ is equal to $I_{bus,in-avg}$. If yes, the converter is operating under steady state condition and the assumed D is the correct value. If not, then the duty ratio is not correct for this operating point and the procedure should be repeated by inputting a different value of D.

3.3 Design curves

In Section 3.2.1, a flowchart was used to illustrate the converter analysis procedure. This procedure can be repeated to determine the intermediate DC bus voltage of the proposed converter for multiple operation points for a range of duty cycles. With the program, which was done in MATLAB for this thesis, steady-state characteristic curves can be generated by varying key parameters.

The proposed converter operating characteristic for any input and output voltage depends on the parameters that used to determine the DC bus voltage, which are:

- Input inductance L_{in}.
- The magnetizing inductance of the two main transformers L_{m1}, L_{m2}.
- The leakage inductance of the two main transformers L_{lk1}, L_{lk2}.
- The turns ratio of the two main transformers, N.

It should be noted that because the proposed converter in this thesis is designed as two identical flyback converters stacked on top of each other so that the value of the converter parameters of the two transformers are identical. For example, if the value of magnetizing inductance L_{m1} of transformer T_1 is varied to generate a characteristic curve, then the same change is applied to L_{m2}. The effect that each of these parameters has on DC voltage bus can be illustrated with graphs of characteristic curves that are generated by varying one parameters and keeping others constant to obtain a steady-state characteristic curve. In the following section, each parameter is discussed individually with respect to the characteristic curves. The relations between parameters are presented with respect to DC bus voltage and duty cycle are presented as they are the most critical parameters.

3.3.1 Design curves of input inductance L_{in}

Two design curves are presented and discussed in this section. Fig. 3.11 shows the effect of varying the input inductor L_{in} on the intermediate DC bus voltage. It can be seen that the DC bus voltage decreases as the input inductor is increased and all the other parameters

are kept constant (except duty cycle which is determined by computer program to achieve the energy equilibrium) at the power range of 0 to 200 watts, as explained in [50].

Fig. 3.12 shows the effect of input inductor L_{in} on duty cycle. It can be seen that all three input inductor values allow the converter to operate in the range of 0 to 0.5. With higher inductor value, the duty cycle has a bigger value and larger range, as explained in [50].

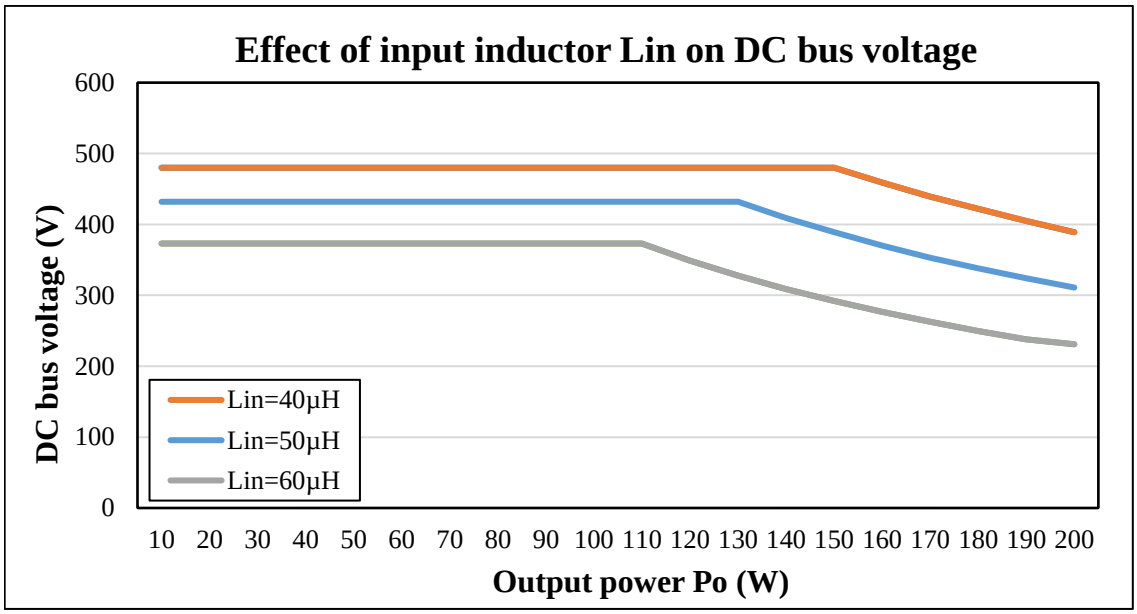

Figure 3.11: Effect of input inductor value $\boldsymbol{L_{in}}$ on DC bus voltage ($\boldsymbol{L_m = 110\mu H, N = 0.5, V_o = 48V, V_{in} = 110AC, f_{sw} = 50kHz}$).

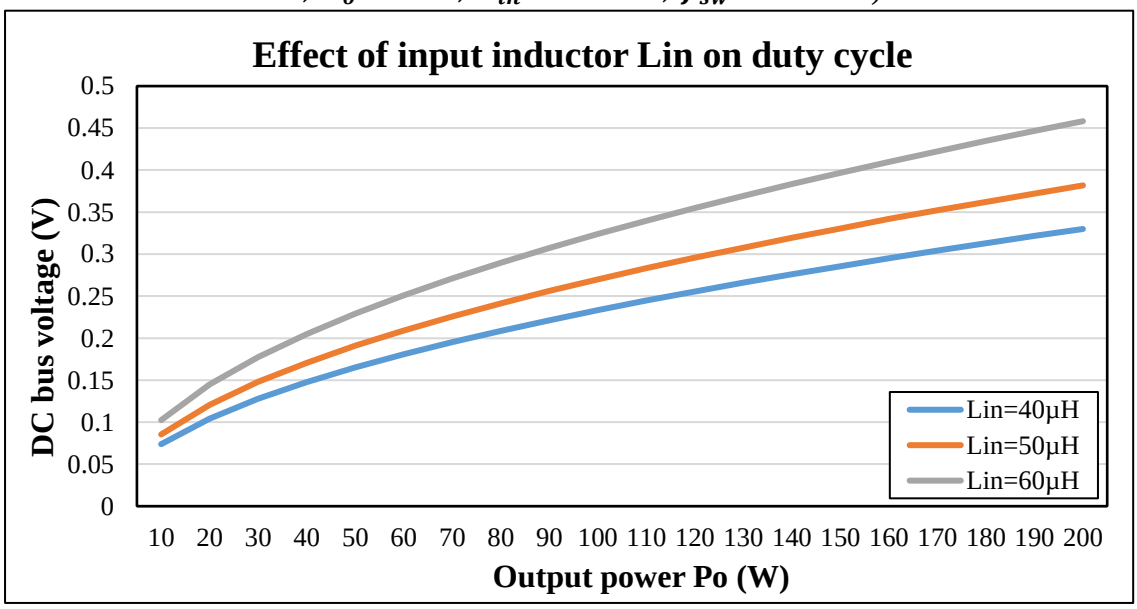

Figure 3.12 : Effect of input inductor value $\boldsymbol{L_{in}}$ on DC bus voltage ($\boldsymbol{L_m = 110\mu H, N = 0.5, V_o = 48V, V_{in} = 110AC, f_{sw} = 50kHz}$).

3.3.2 Design curves of transformer magnetizing inductance L_{m1}, L_{m2}

Two design curves are presented and discussed in this section. Fig. 3.13 shows the effect of varying the value of transformer magnetizing inductance L_m on intermediate DC bus

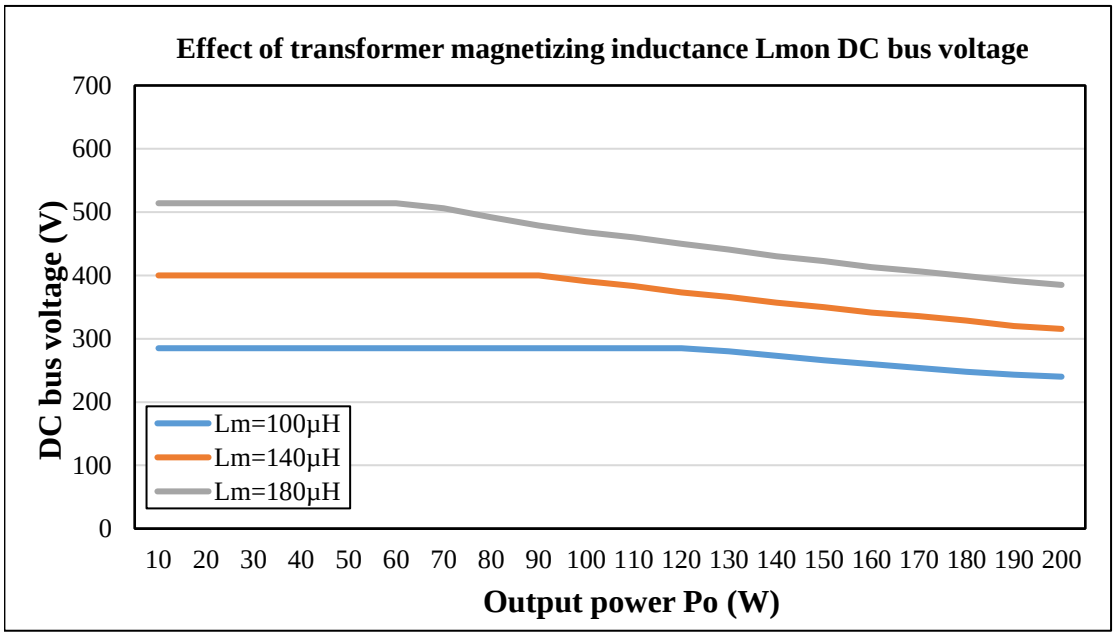

Figure 3.13: Effect of transformer magnetizing inductance value $\boldsymbol{L_m}$ on DC bus voltage ($\boldsymbol{L_{in} = 55\mu H, N = 0.5, V_o = 48V, V_{in} = 110AC, f_{sw} = 50kHz}$).

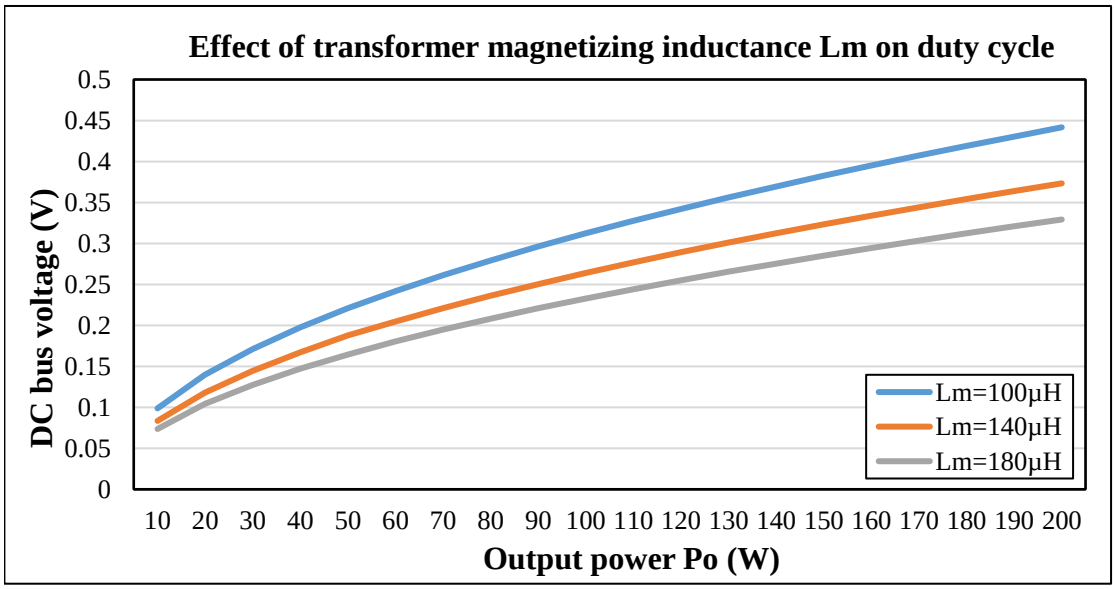

Figure 3.14: Effect of transformer magnetizing inductance value $\boldsymbol{L_m}$ on main switch duty cycle ($\boldsymbol{L_{in} = 55\mu H, N = 0.5, V_o = 48V, V_{in} = 110AC, f_{sw} = 50kHz}$).

voltage. It can be seen that the DC bus voltage increases as the transformer magnetizing inductance is increased with all other parameter are kept constant (except duty cycle). The DC bus voltage is high at light load conditions and low at the full load condition. Fig. 3.14 shows the effect of transformer inductance L_m on duty cycle. It can be seen that the change of duty cycle with a higher value magnetizing inductance is smaller than it is with a lower value which charateristics are explained in [50].

3.3.3 Design curve of transformers turns ratio *N*

A design curve of the effect of the transformer turns ratio *N* on the DC bus voltage is presented and discussed in this section. As can be seen in Fig. 3.15, three different values of transformer turns ratio *N* show that a lower value of *N* results in a higher DC bus voltage at full load condition. In addition, the peak DC bus voltage at different value *N* is the same and happens at light load conditions which charateristics are explained in [50].

3.3.4 Design curves of input voltage V_{in}

Two design curves is presented and discussed in this section. Fig. 3.16 shows the effect of changing the input voltage value V_{in} on the intermediate DC bus voltage. As can be seen in Fig. 3.16, the DC bus voltage increases as input voltage increases with all other

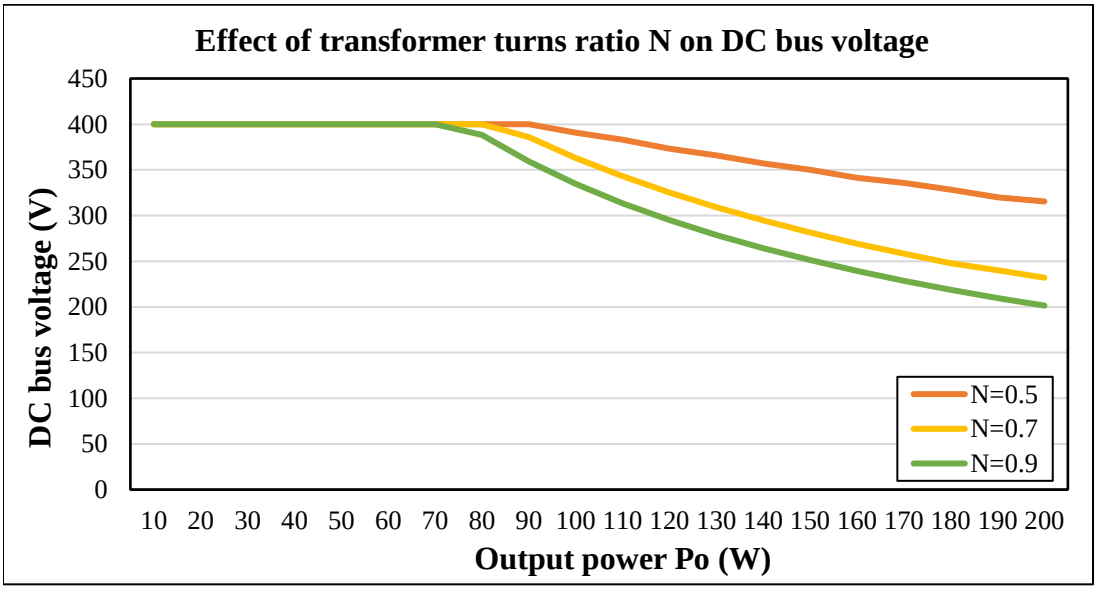

Figure 3.15: Effect of transformer turns ratio *N* on DC bus voltage ($\boldsymbol{L_{in} = 55\mu H}$, $\boldsymbol{L_m = 140\mu H}$, $\boldsymbol{V_o = 48V}$, $\boldsymbol{V_{in} = 110AC}$, $\boldsymbol{f_{sw} = 50kHz}$).

parameter kept constant (except duty cycle). Fig. 3.17 shows the effect of input voltage on duty cycle. As can be seen, the duty cycle increases as input voltage decreases or output power increases which charateristics are explained in [50].

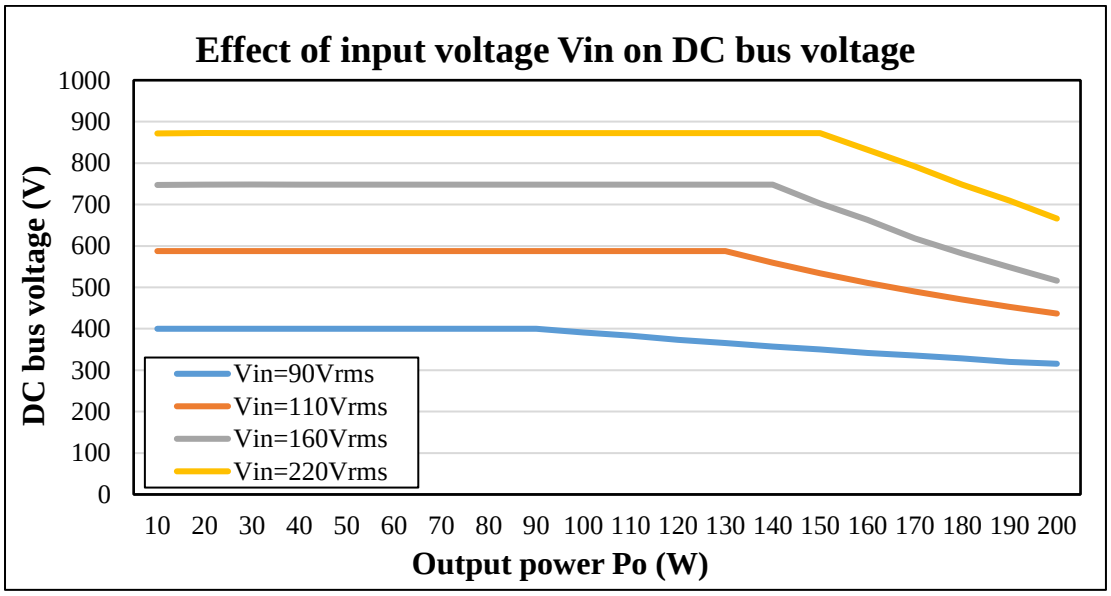

Figure 3.16: Effect of input voltage $\boldsymbol{V_{in}}$ on DC bus voltage ($\boldsymbol{L_{in} = 55\mu H}$, $\boldsymbol{L_m = 140\mu H}$, $\boldsymbol{N = 0.5}$, $\boldsymbol{V_o = 48V}$, $\boldsymbol{f_{sw} = 50kHz}$).

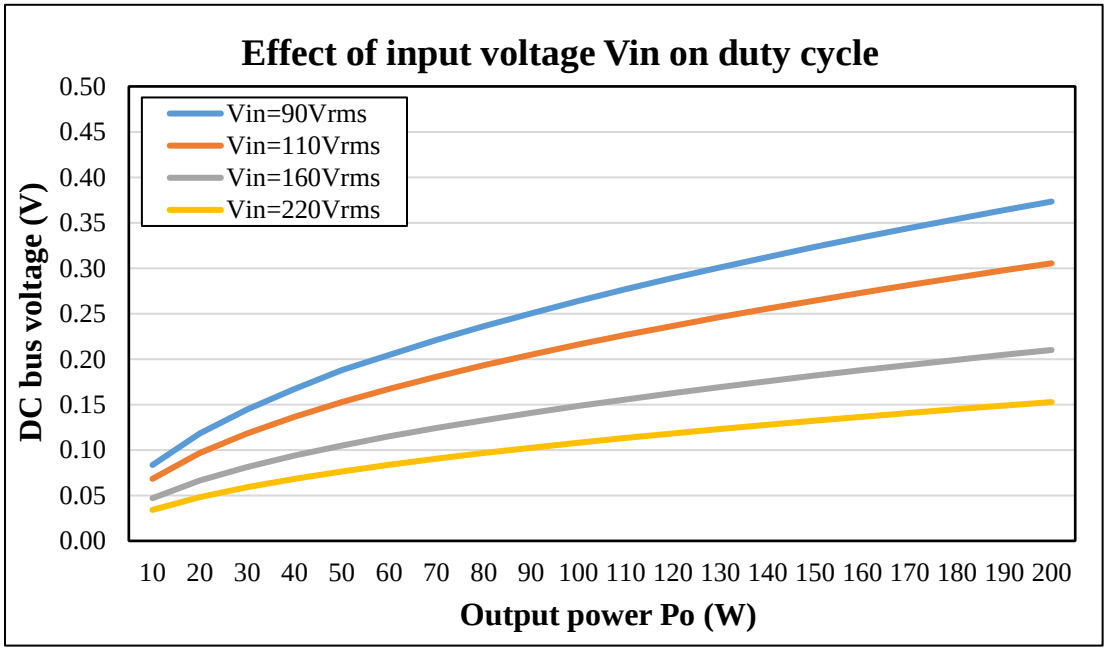

Figure 3.17: Effect of input voltage $\boldsymbol{V_{in}}$ on main switch duty cycle ($\boldsymbol{L_{in} = 55\mu H}$, $\boldsymbol{L_m = 140\mu H}$, $\boldsymbol{N = 0.5}$, $\boldsymbol{V_o = 48V}$, $\boldsymbol{f_{sw} = 50kHz}$).

3.4 Conclusion

In this chapter, a detailed circuit analysis from mathematical equations to design curves was presented. Each mode of converter operation was discussed using simplified equivalent circuit diagrams. The analysis of each mode was based on several mathematical equations that were implemented in a computer program. The computer program was based on the DC bus energy equilibrium, given that single-stage converters do not have control of their DC bus voltage. The computer program was used for determine operation points for the proposed converter, for example, DC bus voltage, duty cycle, etc. Also, it was used to generate design curves for design proposes. From section 3.3.1 to 3.3.5, the effect of different parameters on DC bus voltage was presented with several converter design curves that were generated by the computer program. It should be noted that the proposed converter is a stacked structure so that the DC bus voltage can be split equally among the two DC bus capacitors; therefore, the capacitors and main switches are not exposed to the entire full DC bus voltage but half of it. This advantage gives a greater flexibility in the design of the proposed converter since excessive DC bus voltage places limits on the converter design. This advantage can be used to improve the improvement of single-stage flyback converters.

Chapter 4

4 Converter Design

4.1 Introduction

In the previous chapter, several design curves were generated by using a computer program. Based on these design curves, the effect of key parameters on DC bus voltage and converter duty cycle were analyzed in detail. In this section, a design procedure of proposed converter is presented and is demonstrated with a design example.

4.2 Converter design procedure

A procedure for the design of the proposed converter is presented in this section. The following criteria are used in the procedure:

1) The DC bus voltage should not be excessive. The value of the DC bus voltage should be kept under 800V. For the stacked structure, this voltage is spilt equally on two DC bus capacitors, which is 400V. This consideration reduces the cost of the converter as bulky and expensive capacitors can be avoided.

2) The input line current must satisfy requirements on harmonic content such by regulatory agencies. For this procedure, the IEC1000-3-2 standard is used.

3) There should be enough energy and time to allow current to discharge the output capacitor of the main switches and the active clamp switches so that ZVS operation can be achieved.

4) Excessive input current and magnetizing current should be avoided as losses and stresses are increased if there is high current in the circuit.

With these converter design criteria and the design curves presented in previous section, a design procedure for converter components selection can be established; an example to demonstrate the design procedure is given in this chapter. For the example, the converter is designed according to the following specifications:

1) Input voltage $V_{in} = 90 - 265\ V_{rms}$
2) Output voltage $V_o = 48V$
3) Maximum output power $P_o = 200W$
4) Switching frequency of each main switch $f_{sw} = 50kHz$
5) Active clamp switch switching frequency $f_{sw-aux} = 100kHz$
6) Maximum capacitor voltage: 450V for each capacitor
7) Input current harmonic standard: IEC1000-3-2

The design example will only show the very last result as the procedure is an iterative process which is repeated until a satisfactory result is achieved.

4.2.1 Determine value for main transformer turns ratio N

Transformer turns ratio *N* is an important parameter as it affects the reflected output current at the transformer primary, which discharges the DC bus capacitors. With respect to the design curve in Fig. 3.15, if transformer turns ratio is too low, there will have little current in the primary side to discharge the DC bus capacitor, which results in high DC bus voltage. If *N* is high, the DC bus voltage is decreased, but higher current can result in more conduction losses in the converter's primary side.

For this design example, $N = N_1/N_2 = 0.5$ is chosen to be an appropriate value. With this value, minimum DC bus voltage can be obtained by computer program based on the equation (3.15) to be $V_{bus} = 315V$ at $D = 0.37$, so that $V_{c1} = V_{c2} = 158V$.

4.2.2 Determine value for input inductance L_{in}

The input inductance value should be low enough to ensure that the input current is fully discontinuous under both high-line and low-line operating points. If the input inductance value is too low, however, current in the converter primary side increases. From design curves Fig. 3.11 and Fig. 3.12 mentioned in the previous chapter, the input inductance

needs to be high to reduce the DC bus voltage and to give a larger range for changing the duty cycle. To find a suitable value, the computer program can be run using following equations that are based on the steady-state analysis in Chapter 3:

From the principle of energy equilibrium, the average current inject to the DC bus should be equal to the average current flow to the output

$$I_{bus,in-avg} = I_{bus,out-avg} \tag{4.1}$$

$$\frac{2P_o}{V_{bus}} = f_{ac} \cdot \sum_{k=0}^{n} \frac{D^2 v_{rec}}{4{f_{sw}}^2 L_{in}} \tag{4.2}$$

$$L_{in} = V_{bus} \cdot f_{ac} \cdot \sum_{k=0}^{n} \frac{D^2 v_{rec}}{8 \cdot P_o \cdot {f_{sw}}^2} \tag{4.3}$$

The input inductor value need to ensure that all operation points have fully discontinuous input current. The worst case is when the converter operates with low-line input and full load output. If under this case the input current in the input inductor is fully discontinuous, then same will be true for all other operating points. For the proposed converter, low-line input voltage $V_{in} = 90\,V_{rms}$ and $V_{bus} = 315V$ can be used to determine the input inductor value at the boundary condition for the input section with duty cycle $D = 0.37$ and output power $P_o = 200W$. As a result, L_{in} should be less than $L_{in} = 61.5\mu H$. For the converter design, $L_{in} = 55\mu H$ is selected for this design example.

4.2.3 Determine value for main transformer magnetizing inductance L_m

The magnetizing inductance can be selected according to the design curves in Chapter 3. If value of L_m is too high, the DC bus voltage of the converter becomes excessive. If the value of L_m is too low, then the current in the primary side become excessive, which causes significant conduction losses and lower efficiency.

In Fig. 3.13, it can be seen by changing L_m with selected values of N and L_{in} that the boundary between continuous current mode and discontinuous current mode occurs at a

lighter load when the L_m is increased. For design purposes, the DC bus voltage should be less than 450V for each capacitor at high-line condition. It can be seen from the graph Fig. 3.13 that $L_m = 140\mu H$ is an appropriate value at 220Vrms at $N = 0.5$ and $L_{in} = 55\mu H$.

4.2.4 Determine value for active clamp capacitor V_{clamp}

The design of active clamp capacitor is to ensure that the switches can operate with zero-voltage switching, which is determined by two parameters: the active clamp capacitor and the main transformer leakage inductance. There should be enough energy stored in clamp capacitor C_{clamp} to transfer to the leakage inductance so that the following relation is satisfied:

$$\frac{1}{2} \cdot C_{clamp} \cdot \left(V_{clamp}\right)^2 < \frac{1}{2} \cdot L_{lk} \cdot {I_{in-max}}^2 \tag{4.4}$$

The resonant frequency between clamp capacitor and leakage inductance can be expressed as

$$f_r = \frac{1}{T_r} = \frac{1}{2\pi\sqrt{L_{lk}C_{clamp}}} \tag{4.5}$$

This resonant is significant reduce the conduction losses. It should be note that as proposed converter is stacked structure, the voltage stress of the main switches is half of the DC bus voltage which means that the losses which is the proportional to the square of V_{ds} is low then conventional flyback converter. Before the switch is on, the energy from leakage inductance should completed discharge the output capacitance of the switch and current should go through the body diode. When the current is go through the body diode, there is a short time that the voltage across the switch achieves minimal value. Consider the voltage across the switches is half of the DC bus voltage maximum 450V and current in input inductor 20A, the capacitor value can be selected as 20μF with a design of transformer leakage inductance 9μH.

4.3 Converter specifications

The converter's specification and selected component and parameter values are listed in Tables 1 and 2. Table 1 shows the converter specifications while Table 2 shows the converter parameters. These were used in the construction of an experimental prototype that was used to confirm the operation of the proposed converter. Results obtained from the prototype will be presented in the next chapter.

Table 1: Converter Specifications

Maximum Output Power ($\boldsymbol{P_o}$)	200 W
Input Voltage ($\boldsymbol{V_{in}}$)	90-265 Vrms
Output Voltage ($\boldsymbol{V_o}$)	48 V
AC Line Frequency ($\boldsymbol{f_{ac}}$)	60 Hz
Main Switching Frequency ($\boldsymbol{f_{sw}}$)	50 kHz
Peak Switch Stress ($\boldsymbol{V_{ds-peak}}$)	450V

Table 2: Converter Parameters

Peak Duty Cycle ($\boldsymbol{D_{max}}$)	0.5
Magnetizing Inductance ($\boldsymbol{L_m}$)	140μH
Leakage Inductance ($\boldsymbol{L_{lk}}$)	10μH
Clamp Capacitor ($\boldsymbol{C_{clamp}}$)	10 μF
Transformer Turns Ratio ($\boldsymbol{N = N_2 : N_1}$)	0.5
Auxiliary Winding Turns Ratio ($\boldsymbol{N_r = N_3 : N_1}$)	2
DC Bus Capacitor ($\boldsymbol{C_1, C_2}$)	220 μF
Output Capacitor ($\boldsymbol{C_o}$)	2200 μF
Switches	FQP2N80
Diodes	STPSC1206

4.4 Conclusion

In this chapter, a converter design example that made use of the design curve derived in Chapter 3 was presented. The key converter parameters in the converter are the DC bus voltage and the duty cycle range and all the other converter parameters can be determined once these two parameters have been established. The DC bus voltage cannot be too high as that will introduce high voltage stress in the semiconductors and capacitors, which will increase the converter's cost and converter size. The duty cycle range need to be such that it can satisfy all input conditions and can allow the converter to operate with output 48V for both light load and full load. Other parameters that influence the ZVS range were also discussed as were the trade-offs of each parameter. The converter's specifications and parameters values were summarized at the end in preparation for the next chapter, which will present experimental results that will confirm the feasibility of the proposed converter.

Chapter 5

5 Experimental results

5.1 Introduction

In this chapter, experimental results obtained from a prototype converter are presented to confirm the feasibility of the proposed AC-DC single-stage stacked flyback converter. The converter used in the experimental studies was implemented based on the specifications and design example presented in Chapter 4. Typical experimental waveforms such as input voltage and current, main switch voltage and current will be presented in this chapter and the converter's efficiency will be presented at two input line voltage. At the end, the current harmonic contents of the converter are compared with the IEC1000-3-2 harmonic standard.

5.2 Experimental results

As shown in Fig. 5.1 and Fig. 5.2, a 200W prototype converter was built to verify the proposed converter's feasibility. The prototype parameters and specifications were setup

Figure 5.1 Prototype of the proposed single-stage AC-DC stacked flyback converter (side view).

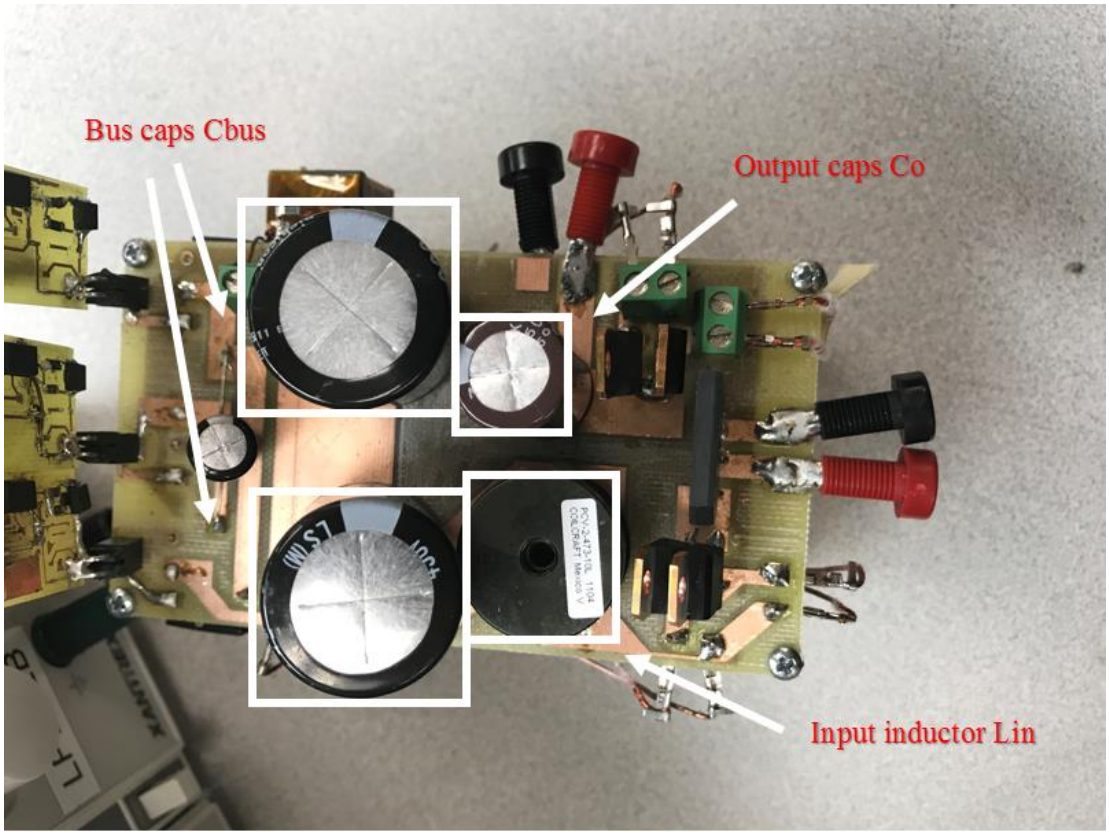

Figure 5.2 Prototype of the proposed single-stage AC-DC stacked flyback converter (vertical view).

in Table. 1 and Table. 2. It should be noted that ensuing converter waveforms were obtained with an 110VAC input voltage for an example operation point. The following key voltage and current waveforms are presented here:

Fig. 5.3(a) shows the input voltage and input current waveforms over several line cycles and Fig. 5.3(b) shows an auxiliary winding current waveform and the input voltage over a couple of switching cycles. It can be seen that input PFC can be achieved and that there no limitation on the conduction angle of the current and that the auxiliary winding current is discontinuous. The measured power factor at this operation point was 0.98.

Fig. 5.3(c) shows typical switch voltage and switch current waveforms during a turn-on switching transition for a main switch. Fig. 5.3(d) shows the same waveforms for the active clamp switch. It can be seen that the converter switches operate with ZVS and the

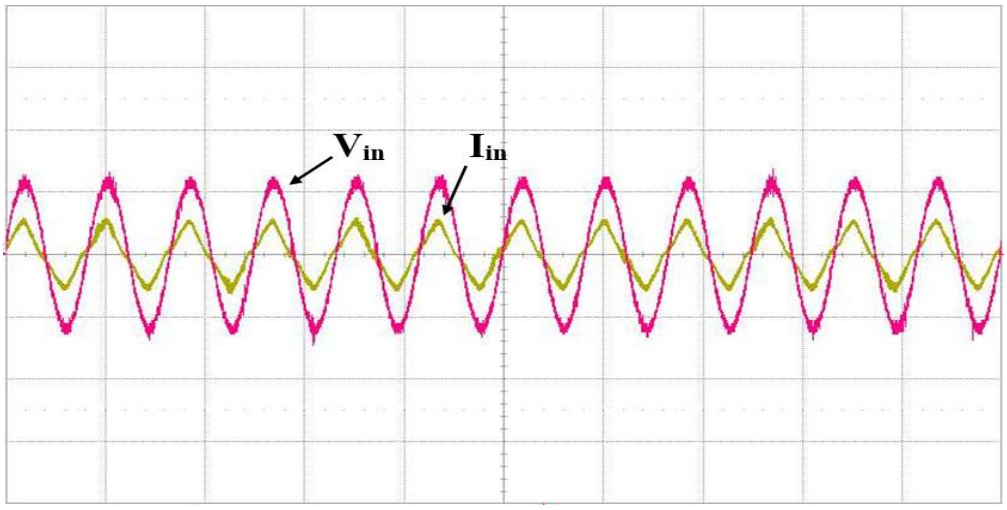

(a)

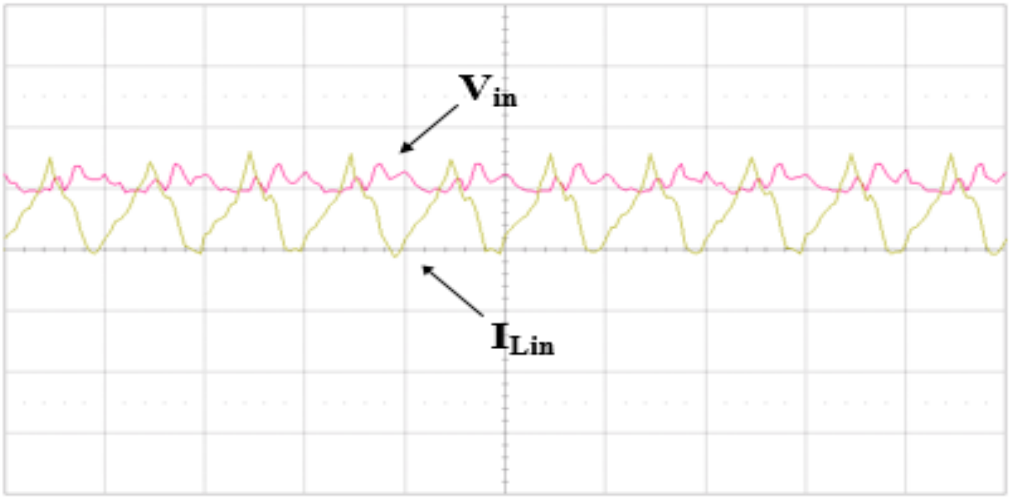

(b)

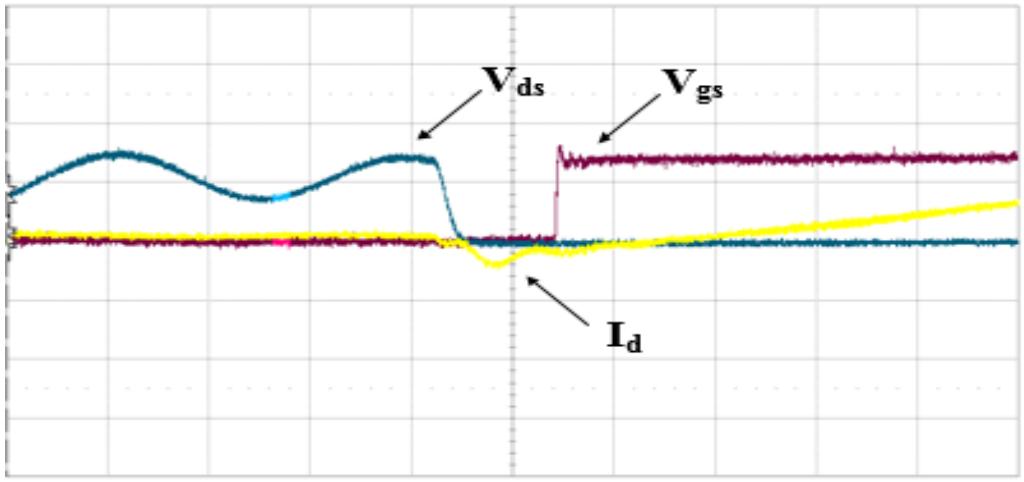

(c)

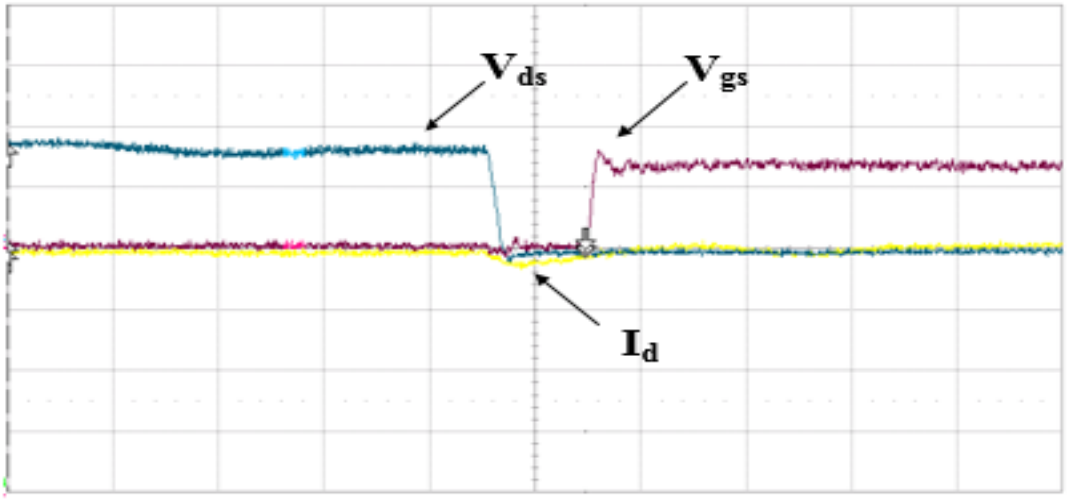

(d)

Figure 5.3 Proposed converter experimental results. (a) Input voltage and current (V: 100 V/div, I: 4 A/div, t: 2ms/div). (b) Input voltage and an auxiliary winding current over a couple of switching cycles (V: 100 V/div, I: 2 A/div, t: 20μs/div). (c) Switch voltage and switch current of the main converter switches ($\boldsymbol{V_{ds}}$: 100 V/div, $\boldsymbol{V_{gs}}$: 10 V/div, I: 2 A/div, t: 500ns/div). (d) ZVS waveforms for the active clamp switch ($\boldsymbol{V_{ds}}$: 100 V/div, $\boldsymbol{V_{gs}}$: 10 V/div, I: 2 A/div, t: 200ns/div).

proposed converter provides an advantage of operating the switches at a reduced voltage stresses, which is half of the DC bus voltage.

5.3 Experimental efficiency

In this section, the measured efficiency is presented to confirm the proposed converter's performance. Fig. 5.4 shows the experimental efficiency of proposed converter at different values of output power at two input line conditions – 110VAC and 220VAC. As can be seen in the graph Fig. 5.4, the proposed converter has higher efficiency at 110VAC than 220VAC, because the high-line voltage condition create higher conduction losses in the converter. converter have higher efficiency at light load condition in both of the high-line and low-line input because the reduced DC bus voltage will create less losses in the semiconductors.

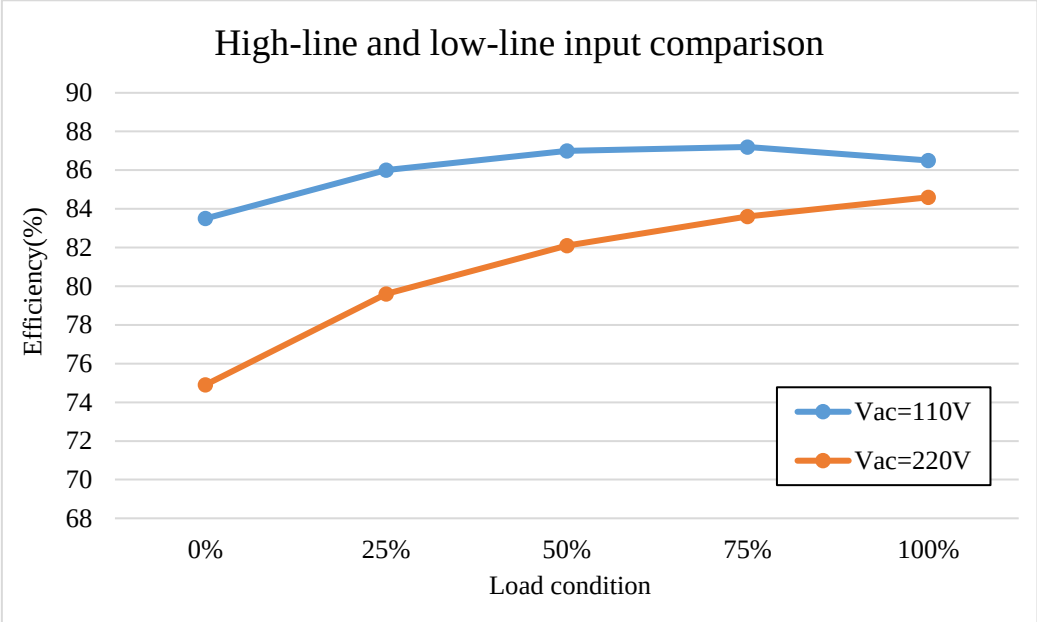

Figure 5.4 Efficiency of two input line voltage at different value of output load condition

5.4 Input current harmonic content

Fig. 5.5 and Fig. 5.6 show the input current harmincs at two input voltage conditions – 110VAC and 220VAC at output power 200W, which was determind to be the worst case

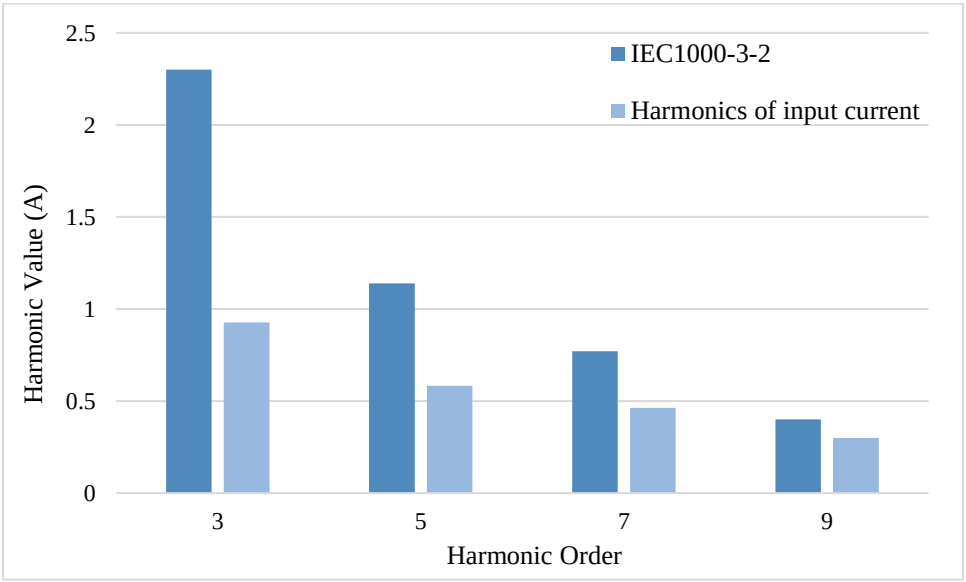

Figure 5.5 Harmonic content of the input current at 220VAC input line and IEC1000-3-2 Class D limitations

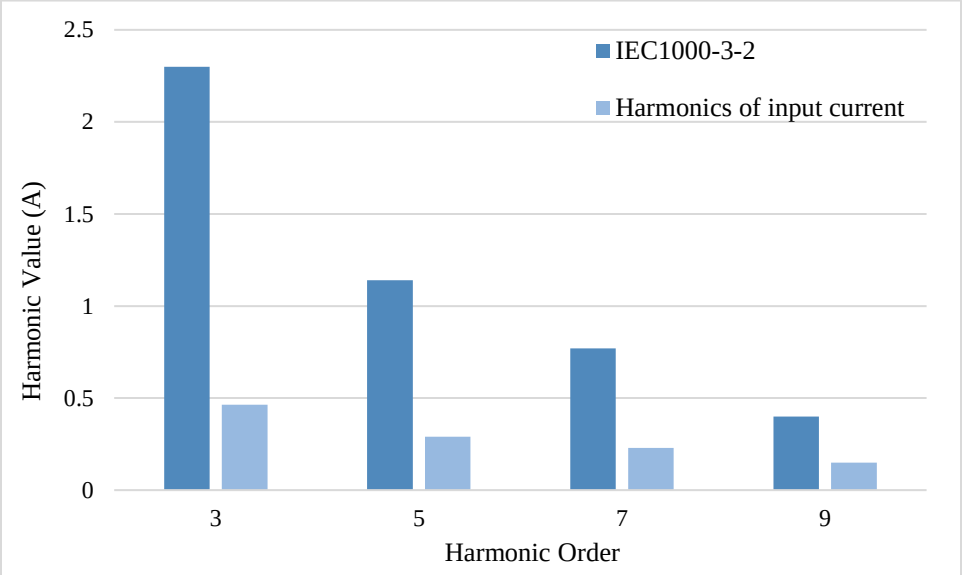

Figure 5.6 Harmonic content of the input current at 110VAC input line and IEC1000-3-2 Class D limitations

condition for the harmonic content of the propose converter. It can be seen that the converter can meet the IEC1000-3-2 Class D standards.

5.5 Conclusion

In this chapter, the performance of a single-phase single-stage AC-DC stacked flyback converter with power factor correction was confirmed with experimental results. From these results, it was confirmed that the zero-voltage switching of both main switches and the active clamp switch can be achieved. High frequency performance of the converter is achieved and high power factor correction operation is proved. The peak voltage stress of each converter is significantly reduced as the each switch only have half of DC bus voltage across it. The efficiency of two input line condition of the proposed AC-DC converter is presented.

Chapter 6

6 Conclusion

6.1 Introduction

In this chapter, the contents of the thesis are summarized, conclusions resulting from the thesis are presented, the contributions of the thesis to the power electronics literature are stated, and suggestions for future work based on the thesis work are given.

6.2 Summary

The main focus of this thesis was to propose a new single-phase single-stage AC-DC stacked flyback converter for low power applications. Since the proposed converter has a stacked structure, it does not have the drawbacks of previously proposed single-stage converters such as high DC bus voltage, high voltage stress on MOSFETs, etc. The stacked converter structure concept thus improves the performance of single-stage AC-DC power supply converters. The contents of this thesis are summarized as follows:

In Chapter 1, basic concepts of power electronics converters related to power factor correction and soft-switching techniques were introduced and a literature review of the state of the art for single-stage AC-DC converters was performed. A number of recently proposed converter topologies were presented and their advantages and drawbacks were demonstrated with particular example converters. The thesis objectives and outline were stated at the end of the chapter.

In Chapter 2, a new single-stage single-phase stacked flyback converter with active clamp zero-voltage switching (ZVS) was presented, its modes of operation were explained and its features were stated. It was shown that the stacked structure concept can be implemented with single-stage modules other than what was used in the proposed converter as long as the modules have magnetic switches. These magnetic switches are auxiliary windings taken from the main power transformer and can be made to behave as ON/OFF switches, depending on when they have voltage across them. Two-terminal input current shapers with magnetic switches can be used as modules in the proposed converter. Three-terminal

input current shapers can be used as well if they have two-terminal equivalents with magnetic switches.

In Chapter 3, the modes of operation of the proposed converter that were presented in Chapter 2 were analyzed mathematically to obtain equations that defined each mode. These equations were then used to develop a computer program that determined viable steady-state operating points. Based on these operating points, graphs of steady-state characteristic curves of key converter parameters that can be used for design purposed were generated. The main principle use in the analysis was the principle of energy equilibrium at the DC bus. The energy pumped from the converter input to the DC bus must be equal to the energy pumped from the DC bus to the output in order for a converter to be in steady state. Valid steady-stage operating points were checked to see if they complied with this principle.

In Chapter 4, a procedure for the design of the proposed converter that used the mathematical equations and design curves that were presented in Chapter 3 was presented and demonstrated with an example. Various trade-offs that need to be considered in the selection of converter components were stated and key component values were selected.

In Chapter 5, an experimental prototype of the proposed converter was built according to the converter specifications in Chapter 4 and results obtained from the prototype converter were presented. These experimental results, including measured efficiency results, further confirmed the feasibility and the advantageous features of the converter. Converter performance on power factor correction and zero-voltage switching were proved by the experimental results.

6.3 Conclusions

The following conclusions can be made based on the result of this thesis:

- Applying the stacked structure concept to the single-phase single-stage AC-DC flyback converters can result in a lower voltage stress (half of the DC bus voltage) on semiconductors.

- The less voltage stress on semiconductors gives greater flexibility in the design of the converter. For example, the input current conduction angle can be extended so that input current distortion is reduced and input power factor is increased.

- The proposed converter can operate with soft-switching using a single active auxiliary switch instead of having to use two auxiliary switches, one for each switch.

- The converter can operate with greater light-load efficiency since CV^2 losses are reduced as the converter switches are exposed to only half the DC bus voltage.

6.4 Contributions

The principal contributions of this thesis are as follows:

- A new single-stage single-phase AC-DC stacked flyback converter with active clamp ZVS was proposed and its operation was explained.

- The steady-state characteristics of the proposed converter were analyzed and graphs of steady-state characteristic curves were generated.

- Design guideline for the proposed converter were presented and a design procedure was derived and demonstrated with a design example.

- The feasibility of the proposed converter was confirmed with a 200W experimental prototype. The efficiency of the proposed converter is presented at high line input and low line input, from light-load to full-load conditions.

6.5 Future work

The following suggestions are made for future work:

- The proposed converter is best suited for maximum 0.5 duty cycle. Research can be done to see if the duty cycle range can be extended to be higher than 0.5, with the operation of the two main switches overlapping.

- The proposed converter used a stacked structure with AC-DC single-stage flyabck converter. Research can be done to see if the stacked structure concept can be used for other types of single-stage AC-DC converters such as forward converters.

References

[1] D. W. Hart, “Power Electronics,” 2011.

[2] Limits for Harmonic Current Emission (Equipment Input Current>16A per Phase), IEC1000-3-2, 1995.

[3] J. Qian and F. C. Y. Lee, "A high-efficiency single-stage single-switch high-power-factor AC/DC converter with universal input," in *IEEE Transactions on Power Electronics*, vol. 13, no. 4, pp. 699-705, Jul 1998.

[4] G. Moschopoulos and P. Jain, "Single-phase single-stage power-factor-corrected converter topologies," in *IEEE Transactions on Industrial Electronics*, vol. 52, no. 1, pp. 23-35, Feb. 2005.

[5] K. I. Hwu and C. F. Chuang, "Applying DSP-based two-stage AC-DC converter to drive SRM with sampling and startup considered," *2009 4th IEEE Conference on Industrial Electronics and Applications*, Xi'an, 2009, pp. 2321-2324.

[6] M. Salehifar, G. Putrus and P. Barras, "Analysis and comparison of conventional two-stage converter and single-stage bridgeless AC-DC converter for off-road battery charger application," *8th IET International Conference on Power Electronics, Machines and Drives (PEMD 2016)*, Glasgow, 2016, pp. 1-7.

[7] M. S. Agamy and P. K. Jain, "An overview of methods to increase the power handling capability of single-stage AC-DC converters," *2011 IEEE International Symposium on Industrial Electronics*, Gdansk, 2011, pp. 147-152.

[8] B. Akın and H. Bodur, "A New Single-Phase Soft-Switching Power Factor Correction Converter," in *IEEE Transactions on Power Electronics*, vol. 26, no. 2, pp. 436-443, Feb. 2011.

[9] M. Mahdavi and H. Farzaneh-Fard, "Bridgeless CUK power factor correction rectifier with reduced conduction losses," in *IET Power Electronics*, vol. 5, no. 9, pp. 1733-1740, November 2012.

[10] C. Qiao and K. M. Smedley, "A topology survey of single-stage power factor corrector with a boost type input-current-shaper," in *IEEE Transactions on Power Electronics*, vol. 16, no. 3, pp. 360-368, May 2001.

[11] S. Li and G. Moschopoulos, "An Ac-Dc Single-Stage PWM Full-Bridge Converter with a Magnetic Switch," *2005 IEEE 36th Power Electronics Specialists Conference*, Recife, 2005, pp. 467-473.

[12] M. Hajiheidari, H. F. Fard and E. Adib, "A single-stage single-switch AC/DC converter using magnetic switch," *2016 24th Iranian Conference on Electrical Engineering (ICEE)*, Shiraz, 2016, pp. 1557-1561.

[13] J. Qian, Q. Zhao and F. C. Lee, "Single-stage single-switch power-factor-correction AC/DC converters with DC-bus voltage feedback for universal line applications," in *IEEE Transactions on Power Electronics*, vol. 13, no. 6, pp. 1079-1088, Nov 1998.

[14] S. Y. Chen, Z. R. Li and C. L. Chen, "Analysis and Design of Single-Stage AC/DC LLC Resonant Converter," in *IEEE Transactions on Industrial Electronics*, vol. 59, no. 3, pp. 1538-1544, March 2012.

[15] H. Ma, Y. Ji and Y. Xu, "Design and Analysis of Single-Stage Power Factor Correction Converter With a Feedback Winding," in *IEEE Transactions on Power Electronics*, vol. 25, no. 6, pp. 1460-1470, June 2010.

[16] S. W. Lee and H. L. Do, "Single-Stage Bridgeless AC–DC PFC Converter Using a Lossless Passive Snubber and Valley Switching," in *IEEE Transactions on Industrial Electronics*, vol. 63, no. 10, pp. 6055-6063, Oct. 2016.

[17] G. G. Pereira, M. F. de Melo, M. A. Dalla Costa and J. M. Alonso, "High-power-factor LED driver based on input current shaper using a flyback converter," *2015 IEEE Industry Applications Society Annual Meeting*, Addison, TX, 2015, pp. 1-6.

[18] S. K. Ki and D. D. C. Lu, "Implementation of an Efficient Transformerless Single-Stage Single-Switch AC/DC Converter," in *IEEE Transactions on Industrial Electronics*, vol. 57, no. 12, pp. 4095-4105, Dec. 2010.

[19] L. Wang, X. Wu and F. Z. Peng, "High input voltage single-stage flyback AC/DC LED driver using series-connected MOSFETs," *2012 Twenty-Seventh Annual IEEE Applied Power Electronics Conference and Exposition (APEC)*, Orlando, FL, 2012, pp. 2379-2384.

[20] Y. Hu, L. Huber and M. M. Jovanovic, "Single-Stage Flyback Power-Factor-Correction Front-End for HB LED Application," *2009 IEEE Industry Applications Society Annual Meeting*, Houston, TX, 2009, pp. 1-8.

[21] A. R. Ghanbari, J. S. Moghani and B. Abdi, "Single-stage soft-switching PFC converter based on DCVM buck and flyback converters," *4th Annual International Power Electronics, Drive Systems and Technologies Conference*, Tehran, 2013, pp. 218-223.

[22] J. P. R. Balestero, F. L. Tofoli, R. C. Fernandes, G. V. Torrico-Bascope and F. J. Mendes de Seixas, "Power Factor Correction Boost Converter Based on the Three-State Switching Cell," in *IEEE Transactions on Industrial Electronics*, vol. 59, no. 3, pp. 1565-1577, March 2012.

[23] G. Moschopoulos, "A simple AC-DC PWM full-bridge converter with integrated power-factor correction," in *IEEE Transactions on Industrial Electronics*, vol. 50, no. 6, pp. 1290-1297, Dec. 2003.

[24] F. Zhang and J. Xu, "A Novel PCCM Boost PFC Converter With Fast Dynamic Response," in *IEEE Transactions on Industrial Electronics*, vol. 58, no. 9, pp. 4207-4216, Sept. 2011.

[25] J. Zhu and A. Pratt, "Capacitor Ripple Current in an Interleaved PFC Converter," in *IEEE Transactions on Power Electronics*, vol. 24, no. 6, pp. 1506-1514, June 2009.

[26] H. S. Athab, D. D. C. Lu and K. Ramar, "A Single-Switch AC/DC Flyback Converter Using a CCM/DCM Quasi-Active Power Factor Correction Front-End," in *IEEE Transactions on Industrial Electronics*, vol. 59, no. 3, pp. 1517-1526, March 2012.

[27] C. Liao and K. M. Smedley, "Design of high efficiency Flyback converter with energy regenerative snubber," *2008 Twenty-Third Annual IEEE Applied Power Electronics Conference and Exposition*, Austin, TX, 2008, pp. 796-800.

[28] A. Mukherjee, M. Pahlevaninezhad and G. Moschopoulos, "A simple flyback microinverter for solar energy systems with variable frequency controlled ZVS," *2013 IEEE Energy Conversion Congress and Exposition*, Denver, CO, 2013, pp. 2026-2031.

[29] N. D. Weise, G. Castelino, K. Basu and N. Mohan, "A Single-Stage Dual-Active-Bridge-Based Soft Switched AC–DC Converter With Open-Loop Power Factor Correction and Other Advanced Features," in *IEEE Transactions on Power Electronics*, vol. 29, no. 8, pp. 4007-4016, Aug. 2014.

[30] C. Li and D. Xu, "Family of Enhanced ZCS Single-Stage Single-Phase Isolated AC–DC Converter for High-Power High-Voltage DC Supply," in *IEEE Transactions on Industrial Electronics*, vol. 64, no. 5, pp. 3629-3639, May 2017.

[31] M. Pahlevaninezhad, P. Das, J. Drobnik, P. K. Jain and A. Bakhshai, "A Novel ZVZCS Full-Bridge DC/DC Converter Used for Electric Vehicles," in *IEEE Transactions on Power Electronics*, vol. 27, no. 6, pp. 2752-2769, June 2012.

[32] Y. Gao, W. Cai and F. Yi, "A single-stage single-phase isolated AC-DC converter based on LLC resonant unit and T-type three-level unit for battery charging applications," *2016 IEEE Applied Power Electronics Conference and Exposition (APEC)*, Long Beach, CA, 2016, pp. 1861-1867.

[33] R. Redl, P. Tenti and J. Daan van Wyk, "Power electronics' polluting effects," in *IEEE Spectrum*, vol. 34, no. 5, pp. 32-39, May 1997.

[34] J. Y. Lee, L. S. Yang, T. J. Liang and M. Y. Cheng, "Analysis and implementation of interleaved single-stage single-phase AC-DC boost-flyback converter," *2009 IEEE 6th International Power Electronics and Motion Control Conference*, Wuhan, 2009, pp. 678-682.

[35] S. Moon, G. B. Koo and G. W. Moon, "A New Control Method of Interleaved Single-Stage Flyback AC–DC Converter for Outdoor LED Lighting Systems," in *IEEE Transactions on Power Electronics*, vol. 28, no. 8, pp. 4051-4062, Aug. 2013.

[36] I. Castro, K. Martin, D. G. Lamar, M. Arias, M. M. Hernando and J. Sebastian, "Single-stage AC/DC dual inductor BCM current-fed push-pull for HB-LED lighting applications," *2016 IEEE Energy Conversion Congress and Exposition (ECCE)*, Milwaukee, WI, 2016, pp. 1-8.

[37] S. Lin, M. Chen, J.. Chen and D. Lin, "Implementation of a single-stage forward-flyback driver with high efficiency and high power factor for LED streetlight," *2017 IEEE 3rd International Future Energy Electronics Conference and ECCE Asia (IFEEC 2017 - ECCE Asia)*, Kaohsiung, 2017, pp. 1078-1083.

[38] H. Dong, X. Xie, L. Jiang, Z. Jin and X. Zhao, "An Electrolytic Capacitor-Less High Power Factor LED Driver Based on a “One-and-a-Half Stage” Forward-Flyback Topology," in *IEEE Transactions on Power Electronics*, vol. 33, no. 2, pp. 1572-1584, Feb. 2017.

[39] H. Athab, A. Yazdani, B. Wu and D. D. C. Lu, "A single-switch single-stage quasi-active PFC converter with bus voltage following peak input voltage," *IECON 2012 - 38th Annual Conference on IEEE Industrial Electronics Society*, Montreal, QC, 2012, pp. 3762-3767.

[40] M. Hajiheidari, H. F. Fard and E. Adib, "A single-stage single-switch AC/DC converter using magnetic switch," *2016 24th Iranian Conference on Electrical Engineering (ICEE)*, Shiraz, 2016, pp. 1557-1561.

[41] F. Alhuwaishel, SinanAl-Obaidi and N. A. Ahmed, "Analysis of quasi-Z source PFC convertor and its comparison with traditional flyback," *2017 IEEE International Workshop On Integrated Power Packaging (IWIPP)*, Delft, 2017, pp. 1-5.

[42] F. Tsai, P. Markowski and E. Whitcomb, "Off-line flyback converter with input harmonic current correction," *Telecommunications Energy Conference, 1996. INTELEC '96., 18th International*, Boston, MA, 1996, pp. 120-124.

[43] Q. T. Nha, C. Y. Lin, M. M. Alam, Y. K. Lo and H. J. Chiu, "Implementation of a single-stage quasi Z-source AC-DC Power Factor Correction converter," *Anti-counterfeiting, Security, and Identification*, Taipei, 2012, pp. 1-5.

[44] K. M. Divya and R. Parackal, "High power factor integrated buck-boost flyback converter driving multiple outputs," *2015 Online International Conference on Green Engineering and Technologies (IC-GET)*, Coimbatore, 2015, pp. 1-5.

[45] T. Alunpipatthanachai, S. Bhatranand and C. Jeraputra, "Design of a single-stage PFC LED driver with a leakage energy recycling circuit," *2016 13th International Conference on Electrical Engineering/Electronics, Computer, Telecommunications and Information Technology (ECTI-CON)*, Chiang Mai, 2016, pp. 1-6.

[46] S. W. Lee and H. L. Do, "Single-Stage Bridgeless AC–DC PFC Converter Using a Lossless Passive Snubber and Valley Switching," in *IEEE Transactions on Industrial Electronics*, vol. 63, no. 10, pp. 6055-6063, Oct. 2016.

[47] X. Chen, T. Jiang, X. Huang and J. Zhang, "A high efficiency bridgeless flyback PFC converter for adapter application," *2013 Twenty-Eighth Annual IEEE Applied Power Electronics Conference and Exposition (APEC)*, Long Beach, CA, 2013, pp. 1013-1017.

[48] L. Huber, Y. Jang and M. M. Jovanovic, "Performance Evaluation of Bridgeless PFC Boost Rectifiers," in *IEEE Transactions on Power Electronics*, vol. 23, no. 3, pp. 1381-1390, May 2008.

[49] M. Narimani and G. Moschopoulos, "A three-level integrated AC-DC converter," *2012 IEEE Energy Conversion Congress and Exposition (ECCE)*, Raleigh, NC, 2012, pp. 2895-2900.

[50] G. Moschopoulos, Mei Qiu, H. Pinheiro and P. Jain, "PWM full-bridge converter with natural input power factor correction," in *IEEE Transactions on Aerospace and Electronic Systems*, vol. 39, no. 2, pp. 660-674, April 2003.

[51] G. Moschopoulos, P. Jain, G. Joos and Yan-Fei Liu, "A single-stage zero-voltage switched PWM full-bridge converter with power factor correction," *Proceedings of APEC 97 - Applied Power Electronics Conference*, Atlanta, GA, 1997, pp. 457-463 vol.1.

[52] Q. Zhao, F. C. Lee and Fu-sheng Tsai, "Voltage and current stress reduction in single-stage power factor correction AC/DC converters with bulk capacitor voltage feedback," in *IEEE Transactions on Power Electronics*, vol. 17, no. 4, pp. 477-484, Jul 2002.

[53] M. S. Agamy and P. K. Jain, "A Three-Level Resonant Single-Stage Power Factor Correction Converter: Analysis, Design, and Implementation," in *IEEE Transactions on Industrial Electronics*, vol. 56, no. 6, pp. 2095-2107, June 2009.

[54] E. H. Ismail, A. J. Sabzali and M. A. Al-Saffar, "Buck–Boost-Type Unity Power Factor Rectifier With Extended Voltage Conversion Ratio," in *IEEE Transactions on Industrial Electronics*, vol. 55, no. 3, pp. 1123-1132, March 2008.

[55] X. Xie, J. Li, K. Peng, C. Zhao and Q. Lu, "Study on the Single-Stage Forward-Flyback PFC Converter With QR Control," in *IEEE Transactions on Power Electronics*, vol. 31, no. 1, pp. 430-442, Jan. 2016.

[56] W. Wu, W. Qiu, K. Rustom, S. Luo and I. Batarseh, "Efficient high power factor single-stage AC/DC converter," *2002 IEEE 33rd Annual IEEE Power Electronics Specialists Conference. Proceedings (Cat. No.02CH37289)*, 2002, pp. 1143-1148.

[57] Gwan-Bon Koo and Myung-Joong Youn, "A new zero voltage switching active clamp flyback converter," *2004 IEEE 35th Annual Power Electronics Specialists Conference (IEEE Cat. No.04CH37551)*, 2004, pp. 508-510 Vol.1.

[58] A. Lazaro, A. Barrado, M. Sanz, V. Salas and E. Olias, "New Power Factor Correction AC-DC Converter With Reduced Storage Capacitor Voltage," in *IEEE Transactions on Industrial Electronics*, vol. 54, no. 1, pp. 384-397, Feb. 2007.

[59] R. Watson, F. C. Lee and G. C. Hua, "Utilization of an active-clamp circuit to achieve soft switching in flyback converters," in *IEEE Transactions on Power Electronics*, vol. 11, no. 1, pp. 162-169, Jan 1996.

[60] K. Schenk and S. Cuk, "A single-switch single-stage active power factor corrector with high quality input and output," *PESC97. Record 28th Annual IEEE Power Electronics Specialists Conference. Formerly Power Conditioning Specialists Conference 1970-71. Power Processing and Electronic Specialists Conference 1972*, St. Louis, MO, 1997, pp. 385-391 vol.1.

[61] J. Wei, K. Yao, M. Xu and F. C. Lee, "Applying transformer concept to nonisolated voltage regulators significantly improves the efficiency and transient response," *Power Electronics Specialist Conference, 2003. PESC '03. 2003 IEEE 34th Annual*, 2003, pp. 1599-1604 vol.4.

[62] G. Moschopoulos, Yan Liu and Sondeep Bassan, "AC-DC quasi-single-stage converters," *INTELEC 07 - 29th International Telecommunications Energy Conference*, Rome, 2007, pp. 498-505.

[63] G. Moschopoulos and Y. Zheng, "Buck-Boost Type Ac-Dc Single-Stage Converters," *2006 IEEE International Symposium on Industrial Electronics*, Montreal, Que., 2006, pp. 1123-1128.

[64] M. T. Madigan, R. W. Erickson and E. H. Ismail, "Integrated high-quality rectifier-regulators," in *IEEE Transactions on Industrial Electronics*, vol. 46, no. 4, pp. 749-758, Aug 1999.

[65] Bor-Ren Lin, Huann-Keng Chiang, Kao-Cheng Chen and David Wang, "Analysis, design and implementation of an active clamp flyback converter," *2005 International Conference on Power Electronics and Drives Systems*, Kuala Lumpur, 2005, pp. 424-429.

[66] Y. M. Liu and L. K. Chang, "Single-Stage Soft-Switching AC–DC Converter With Input-Current Shaping for Universal Line Applications," in *IEEE Transactions on Industrial Electronics*, vol. 56, no. 2, pp. 467-479, Feb. 2009.

[67] D. G. Lamar, J. S. ZÚÑiga, A. R. Alonso, M. R. GonzÁlez and M. M. Hernando Álvarez, "A Very Simple Control Strategy for Power Factor Correctors Driving High-Brightness LEDs," in *IEEE Transactions on Power Electronics*, vol. 24, no. 8, pp. 2032-2042, Aug. 2009.

[68] N. Vazquez, J. Lopez, J. Arau, C. Hernandez and E. Rodriguez, "A different approach to implement an active input current shaper," in *IEEE Transactions on Industrial Electronics*, vol. 52, no. 1, pp. 132-138, Feb. 2005.

[69] J. Sebastian, A. Fernandez, P. J. Villegas, M. M. Hernando and M. J. Prieto, "New active input current shapers to allow AC-to-DC converters with asymmetrically driven transformers to comply with the IEC-1000-3-2," in *IEEE Transactions on Power Electronics*, vol. 17, no. 4, pp. 493-501, Jul 2002.

[70] D. L. O'Sullivan, M. G. Egan and M. J. Willers, "A novel single-stage off-line converter with PFC, fast output voltage regulation and reduced switching frequency range," *2000 Eighth International Conference on Power Electronics and Variable Speed Drives (IEE Conf. Publ. No. 475)*, London, 2000, pp. 286-292.

[71] X. Wu, G. Hua, J. Zhang and Z. Qian, "A New Current-Driven Synchronous Rectifier for Series–Parallel Resonant (LLC) DC–DC Converter," in *IEEE Transactions on Industrial Electronics*, vol. 58, no. 1, pp. 289-297, Jan. 2011.

[72] R. Beiranvand, B. Rashidian, M. R. Zolghadri and S. M. H. Alavi, "Using LLC Resonant Converter for Designing Wide-Range Voltage Source," in *IEEE Transactions on Industrial Electronics*, vol. 58, no. 5, pp. 1746-1756, May 2011.

[73] C. H. Chang, C. A. Cheng, H. L. Cheng and C. F. Lin, "Analysis and design of a novel interleaved single-stage LLC resonant AC-DC converter," *2013 IEEE 10th International Conference on Power Electronics and Drive Systems (PEDS)*, Kitakyushu, 2013, pp. 602-607.

Curriculum Vitae

Name: Yuntong Li

Post-secondary Education and Degrees:

Beijing Jiaotong University
Beijing, China
2010-2012 B.Eng.

The University of Manchester
Manchester, United Kingdom
2012-2014 B.Eng.

The University of Western Ontario
London, Ontario, Canada
2015-2017 M.A.Sc.

Related Work Experience

Teaching Assistant
The University of Western Ontario
2015-2016

Publications:

Y. Li and G. Moschopoulos, "State of the art low power AC-DC single-stage converters," *in Proc. IEEE Telecommunications Energy Conference (INTELEC)*, 2017.

Y. Li and G. Moschopoulos, "A new single-phase single-stage AC-DC stacked flyback converter with active clamp ZVS," *in Annual IEEE Applied Power Electronics Conference and Exposition (APEC)*, 2018.